366

GUIDE FOR PARTIAL DISCHARGE MEASUREMENTS

IN COMPLIANCE TO IEC 60270

Working Group
D1.33

December 2008

WG D1.33

Guide for Partial Discharge measurements in compliance to IEC 60270

Author		**Co-Authors**	
Eberhard Lemke	Germany	Sonja Berlijn	Sweden
		Edward Gulski	Netherland
		Michael Muhr	Austria
		Edwin Pultrum	Netherland
		Thomas Strehl	Germany
		Wolfgang Hauschild	Germany
		Johannes Rickmann	France
		Guiseppe Rizzi	Italy

ISBN: 978-2-85873-053-7

TABLE OF CONTENTS

1 INTRODUCTION

The first standard for the detection of partial discharges (PD) in high-voltage apparatus was issued in 1940 by the National Electrical Manufacturers Association (NEMA) [1] which refers to "Methods of Measuring Radio Noise". The NEMA Publication 107 "Methods of Measurement of Influence Voltage (RIV) of High-Voltage Apparatus", edited in 1964, was an extensive revision of the former publication. First practical experiences with the RIV method revealed that besides corona discharges ignited on HV electrodes in ambient air also internal discharges in solid and liquid dielectrics could be recognized. Therefore, an equivalent method for measuring radio interference voltages was introduced also in Europe by the Comité International Spécial des Perturbation Radioélectrique (CISPR) in 1961 [3 and 4].

The measurement of radio interference voltages expressed in terms of μV, however, is weighted according to the acoustical noise impression of the human ear, which is not correlated to the PD activity in HV apparatus [5and 6]. Therefore a conversion factor between μV and pC cannot be expected in general [5 and 6]. A further back draw of the RIV method is the strong impact of the mid-band frequency and the band-width as well as the PD pulse repetition rate on the reading. As a consequence, the IEC Technical Committee No. 42 decided the issue of a separate standard on the measurement of partial discharges associated with the PD quantity apparent charge expressed in terms of pC.

The first edition of IEC Publication 270 appeared in 1968 [7]. Besides the definition of the apparent charge as well as the PD inception and extinction voltage several other quantities were introduced, such as the repetition rate, the energy and the power of PD pulses. Additionally, rules for the calibration of the apparent charge were specified and guidelines were presented for the identification of the most typical PD sources using an oscilloscope for displaying phase-resolved PD pulse sequences along each AC cycle versus either the elliptical or the linear time base.

The second edition of IEC Publication 270 appeared in 1981 [8]. This document was only a small revision of the first issue. However, it contained more details on the calibration procedure. Additionally, the PD quantity "largest repeatedly occurring apparent charge" was introduced. Since that time electrical PD measurements have been proven as an indispensable tool to trace dielectric imperfections, which may be caused either by poor assembling work or by design failures of HV apparatus. Therefore, the increased quality requirements for modern HV insulation systems as well as the enhancement of the electrical field strength and last but not least the desired enlargement of the lifetime of HV equipment requires not only an early detection of severe PD defects but also reproducible and comparable test results. As a consequence, the third publication of IEC 60270 [9] issued in 2000 revised extensively the second edition of 1981. The current standard covers besides the conventional analogue instrumentation also digital instruments for a more complex acquisition and analysis of the captured PD data. Specific problems arising for PD tests under DC voltages or superimposed AC and DC voltages are also considered. Moreover, a clause on maintaining the characteristics of PD measuring systems and PD calibrators is added, where the "Record of Performance (RoP)" shall include not only information on nominal characteristics of the PD measuring facility but also results of type, routine and performance tests as well as results of performance checks.

For better understanding the background of the current IEC Publication 60270 [9] the CIGRE Working Group D1.33 "High-Voltage Testing and Measuring Techniques" decided to summarize the state of the art of conventional electrical PD measurements in a Technical Brochure which is intended as a guide for engineers dealing with quality assurance PD tests of HV apparatus. Based on a brief review of the history of PD detection first some fundamentals of the PD occurrence will be highlighted in this brochure. Based on that essential criteria for the design of PD measuring circuits and PD calibrators will be discussed. In this context it should be noted that currently the standard IEC 62478 [10] is under preparation, which covers the non-conventional electromagnetic and acoustical PD detection methods. These topics, however, are outside of the scope of this brochure and will thus not be considered here in more detail.

2 History OF PD RECOGNITION

Looking back to the very beginning of PD recognition we should remind that discharges on dielectric surfaces have been invented already in 1777 by G. Ch. Lichtenberg [11]. However, it was almost 100 years later when it could be clarified that the Lichtenberg dust figures manifest electrical discharge channels on the surface of dielectrics [12-20]. Nowadays this very old technique is also utilized, in particular in combination with electrical methods for fundamental studies of the discharge physics [21-23].

Since the beginning of the last century, when the high voltage technology was introduced for electrical power generation and transmission systems, discharges have already been recognized as a harmful source for the insulation ageing in HV apparatus as reported, for instance, in [24-30]. At that time the term "corona discharge" has generally been used instead of the nowadays standardized term "partial discharge".

Forced by the rapidly increasing HV transmission voltage level, which required a substantial improvement of insulating materials, the first facilities for electrical PD recognition were introduced at the beginning of the last century [31-36]. Using such instruments for fundamental PD studies the knowledge on partial discharges could be improved continuously, as reported, for instance, in [37-67]. Due to the rising experience in PD recognition the first industrial PD detectors were developed in the middle of the last century [68-72] which contributed essentially to further achievements in the PD detection technology [73-102].

In the 1970´s, when extruded materials were introduced for the insulation of power cables, the measurement of a PD level down to the pC range was demanded, because PD´s of few pC may already lead to an inevitable breakdown of polymeric insulations. This forced the development of improved PD measuring systems capable also for the localization of the PD site in long power cables [103-109]. Moreover, PD tests in compliance to IEC 60270 [9] were increasingly applied for quality assurance tests of power transformers [110-130]. In this context it seems noticeable that PD tests of gas-insulated switchgears (GIS) are performed since the seventies. With respect to an effective rejection of electromagnetic noises instead of the standardized IEC method the non-conventional electromagnetic (UHF) and acoustical methods are increasingly utilized, which are the objective of the new standard IEC 62478 [10] and will thus not be considered here.

Since the 1970´s conventional analogue instruments were increasingly substituted by more powerful digital systems in order to fulfill the rising scientific and technical interest in the stochastic PD nature. Initially multi-channel pulse-height analysers were applied [131-133]. Few years later this technique was substituted by computerized PD measuring systems capable for processing, acquisition and phase-resolved visualization of the very complex PD data [134-160]. Nowadays the digital PD measurement technique is common practice in the laboratory and in the field. Moreover, the classical analogue procedures for noise rejection [161-168] are substituted increasingly by more effective digital de-noising tools [169-180].

It should be noted here that standardized electrical PD measurements for quality assurance tests in laboratory have well been proven also for on-site PD diagnostics of HV apparatus, such as power cables [181-188] as well as for electrical machines and power transformers [189-212]. Based on practical experience obtained by such field tests, important knowledge rules were created and published in 2003 by the CIGRE Joint TF 15.11/33.03.02 [213].

Aspects of PD diagnosis of HV apparatus in service as well as tools for the de-noising of PD signals and the interpretation of PD test results, however, are outside of the scope of the standard IEC 60270 [9] and will thus not be considered in this Technical Brochure.

3 PD OCCURRENCE

In technical insulations PD are generally caused by imperfections. Due to the created space charge the PD occurrence depends on the local field strength in the vicinity of the imperfection as well as on the type of the applied test voltage, such as continuous AC and DC voltages as well as transient switching and lightning impulse voltages. The standard IEC 60270 [9] refers generally to PD measurements of electrical apparatus, components or systems tested with AC voltages up to 400 Hz. Only a short part refers also to the particularities of PD tests under DC voltages. This Technical Brochure, however, deals exclusively with the PD occurrence under power frequency test voltages. The design of PD measuring circuits as well as the interpretation of PD test results requires a sufficient understanding of the very complex PD phenomena. Therefore, in the following section essential particularities of the PD occurrence will be summarized, where the various topics are treated in a highly simplified manner, because a more exhaustive treatment would exceed the scope of this brochure.

Classification of PD Events

From a physical point of view self-sustaining electron avalanches may be created only in gases. Consequently, discharge in solid and liquid dielectrics may occur only in gaseous inclusions, such as voids or cracks in solid materials as well as gas bubbles in liquids. Therefore, PD phenomena occurring in ambient air, such as glow, streamer and leader discharges, may also happen in gaseous inclusions. The pulse charge created by glow discharges, often referred to as Townsend discharges, is usually in the order of few pC. Streamer discharges create pulse charges between about 10 pC and some 100 pC. A transition from streamer to leader discharges may occur if the pulse charge exceeds few 1000 pC.

Partial discharges are ignited generally if the electrical field strength inside the gaseous inclusion exceeds the intrinsic field strength of the gas. In technical insulation PD events are the consequence of local field enhancements due to imperfections. Therefore, partial discharges are defined in IEC 60270 [9] as:

> *"localized electrical discharges that only partially bridges the insulation between conductors and which can or cannot occur adjacent to a conductor. Partial discharges are in general a consequence of local electrical stress concentrations in the insulation or on the surface of the insulation. Generally, such discharges appear as pulses having a duration of much less than 1 µ.s"*

From a technical point of view it can be distinguished between the following two major kinds of discharges:

1. External partial discharges

Partial discharges in ambient air are generally classified as "external discharges" often referred to as "corona-discharges". Close to the inception voltage first glow and streamer discharges may appear (Fig. 1a). Stable leader discharges may only occur in very long air gaps exceeding the meter-range. Although chemical processes are excited by gas discharges, the created by-products are continuously substituted by the circulating gas. Therefore discharge processes in pure ambient air can be considered as reversible and thus as harmless in general. External discharges in ambient air propagating along solid dielectric surfaces, however, may become harmful because may they create irreversible degradation processes. Due to normal and tangential field vectors leader-like discharges can be ignited, often referred to as "Toepler discharges" or "gliding discharges". Such discharge types may bridge very long gap distances, even if the test voltage level is raised only few kV above the leader inception voltage. Additionally, the solid insulation surface may be eroded progressively due to the local high temperature in the propagating leader channels.

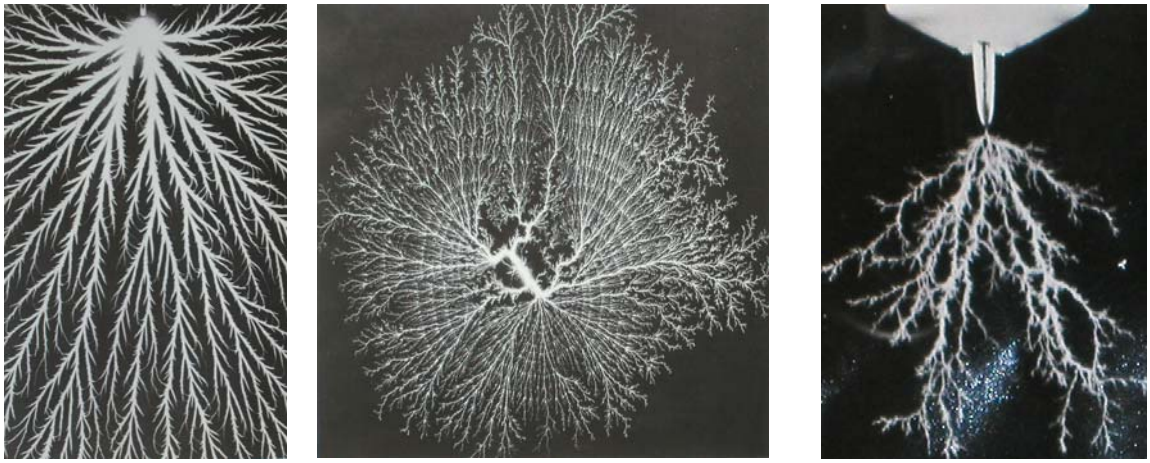

a) Streamer discharge in air [21] b) Leader discharge in oil [22] c) Treeing in PMMA [59]

Fig. 1: Photographs of typical PD channels

Considering technical insulation systems reversible external discharges in air are representative, for instance, for grading rings of insulators used for HV transmission lines as well as for screening electrodes used for HV test facilities. Irreversible gliding discharges may be ignited on transformer bushings and on power cable terminations due to local imperfections of the field grading.

2. Internal discharges

Partial discharges due to imperfections in insulating liquids (Fig. 1b) and solid dielectrics (Fig. 1c) as well as in compressed gas are classified as internal discharges. As mentioned previously, self-sustaining electron avalanches are only created in gaseous inclusions. Thus discharges in solid insulations may only be ignited in gas-filled cavities, such as voids and cracks or even in defects of the molecular structure. In liquid insulations partial discharges may appear in gas-bubbles due to thermal and electrical phenomena and in water-vapour which may be created in high field regions.

The PD inception and extinction voltage as well as the PD magnitudes and the phase-resolved PD patterns are governed not only by the type of the defect and the pressure inside the gas-filled cavities but also by the geometrical size, as illustrated in Fig. 2. Because internal discharges cause a progressive insulation ageing they are often classified as irreversible.

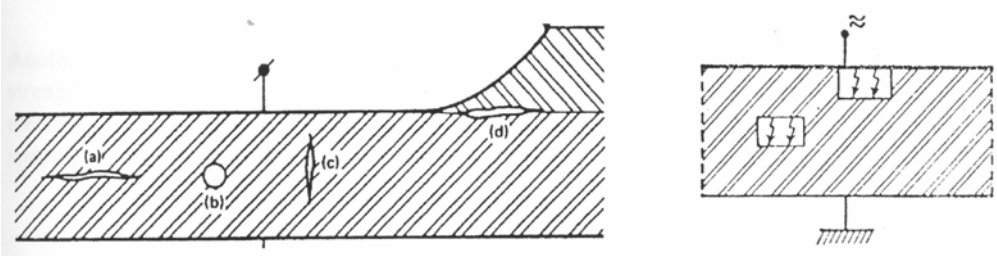

Fig. 2: Typical sizes of gaseous inclusions in solid dielectrics [50, 65]

In technical insulation internal discharges are representative, for instance, for XLPE power cables and cast-resin insulated instrument and power transformers. Here so-called electrical trees (see Fig. 1c) may propagate either very fast or extremely slowly. Therefore a breakdown may happen within few seconds or it may last years until the ultimate breakdown occurs. Internal discharges may also appear between interfaces of solid

and liquid dielectrics and could become harmful if "gliding" along the surface of solid dielectrics. Internal discharges in gas-insulated switchgears (GIS), which are usually ignited by fixed or free-moving particles, have also to be estimated as very harmful, because they may dissociate the SF_6 gas into by-products. This can deteriorate solid insulation materials or create poison resulting in dangerous substances which may trigger an ultimate breakdown forced by transient over-voltages.

Time parameters of PD current pulses

For better understanding the requirements for PD measuring circuits, knowledge of the characteristic parameters of original PD pulses is necessary. These can be measured accurately if the "inverted" point to plane gap is used, i.e. the plane electrode is connected to the HV test supply and the needle electrode is grounded via a measuring resistor R_m, as illustrated in the figures 3 to 5.

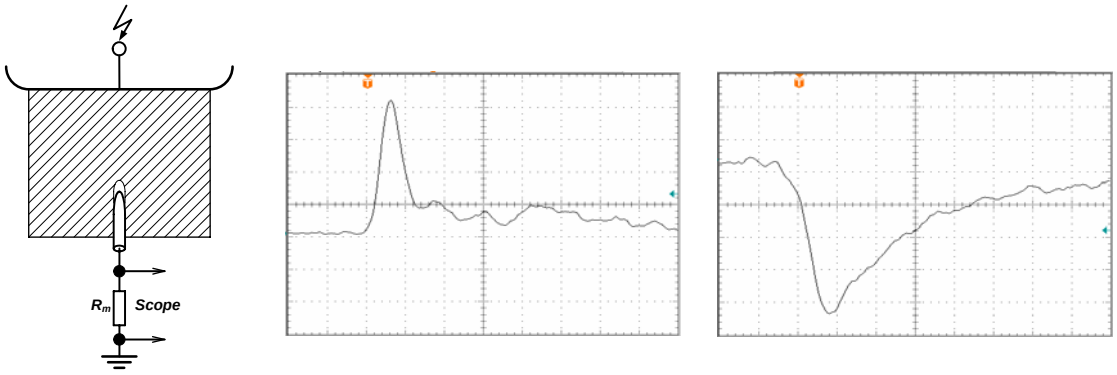

scale: 0.8 mA/div, 2 ns/div scale: 0.2 mA/div, 2 ns/div

Fig. 3: Positive and negative PD current pulses of a cavity discharge in XLPE

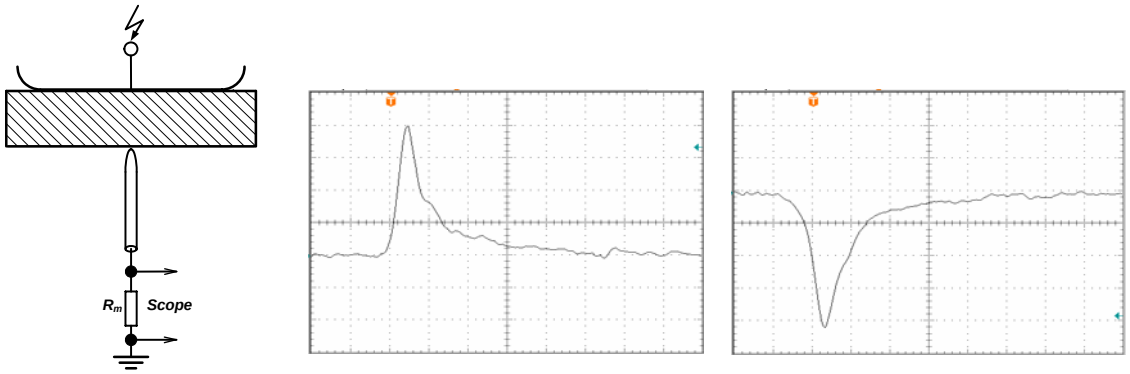

scale: 0.8 mA/div, 2 ns/div scale 0.2 mA/div, 2 ns/div

Fig. 4: Positive and negative PD current pulses of a gliding discharge

Without going into details it can be stated that most of the original PD pulses are characterized by a duration in the nanosecond range, as first calculated by Bailey [53] in 1966 and confirmed experimentally by Fujimoto and Boggs by means of the first available 1000 MHz oscilloscope in 1981[61]. The pulse duration time, however, may scatter over a wide range [67], as illustrated exemplarily for void discharges in Fig. 6 and for gliding discharges in Fig. 7. The significant time parameters of PD pulses depend on the gas pressure and the size of the gaseous inclusion as well as on the kind and magnitude of the applied test voltage and the stressing

time. Negative discharges in air, however, often referred to as “Trichel-pulses”, are characterized by an almost constant duration in the order of 150 ns, see Fig. 5.

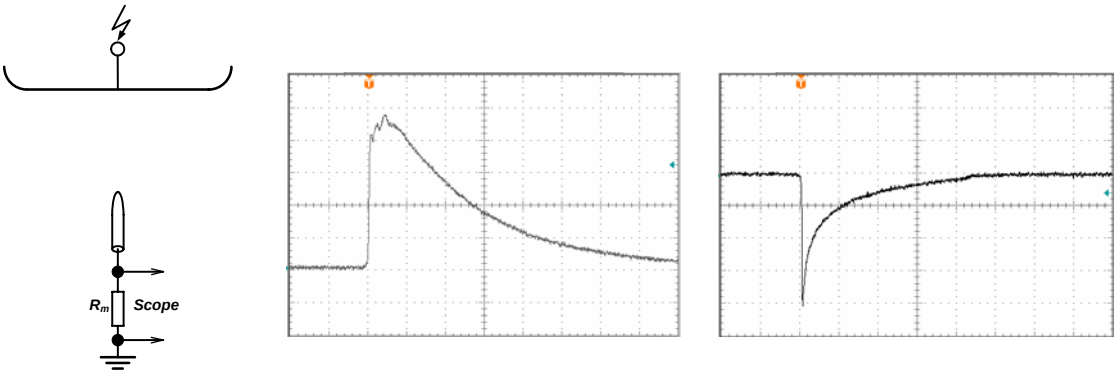

scale: 4 mA/div, 4 ns/div scale: 0.8 mA/div, 40 ns/div

Fig. 5: Positive and negative PD current pulses of a discharge in ambient air

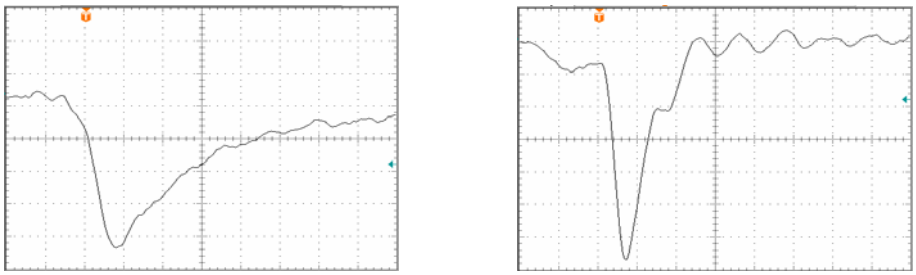

scale: 0.2 mA/div, 2 ns/div scale: 0.8 mA/div, 2 ns/div

Fig. 6: Negative PD current pulses of a void discharge in XLPE at the very beginning (left) and 30 minutes after applying the AC test voltage (right)

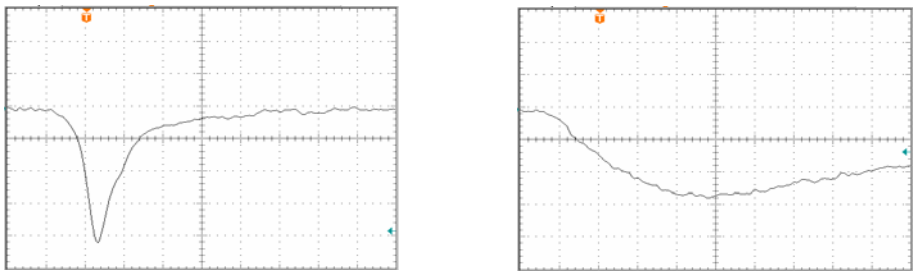

scale: 0.8 mA/div, 2 ns/div scale: 0.8 mA/div, 2 ns/div

Fig. 7: Negative PD current pulses of a gliding discharge at the very beginning (left) and 30 minutes after applying the AC test voltage (right)

In this context it seems important to note that the shape of original PD current pulses occurring in technical insulation cannot be measured directly because the PD source is not accessible by a measuring probe as in the case of the inverted needle-plane arrangement. That means the PD transients in HV apparatus are only detectable via the terminals of the test object. **Consequently, only a small fraction of the pulse charge originated at the PD site is measurable.** Therefore, critical values for PD quantities specified in the relevant standards for quality assurance tests of HV apparatus are not based on the physics of PD phenomena but on long-term experiences of experts.

Moreover it has to be taken into consideration that the current pulses propagating from the PD site to the terminals of the test object may be distorted extremely, where the pulse amplitude is attenuated and the pulse duration is elongated. Additionally, oscillations may also be excited. In many cases, however, the current-time integral and thus the pulse charge remains nearly invariant. **As a consequence, not the peak value of the of PD current captured from the test object terminals but the current-time integral, i.e. the pulse charge, is the most suitable PD quantity for a quantitative evaluation of the PD intensity**, as will be presented more in detail in the following.

Phase-resolved PD patterns

The advantage of measuring the pulse charge is not only its invariance but also its much longer duration if compared to origin PD pulses. Therefore, characteristic PD signatures can simply be displayed versus one cycle of the power frequency AC test voltage by means of an oscilloscope, using a time base which covers the time duration of one 50 Hz cycle, i.e.20 ms. Such records cannot be achieved for sequences of original PD pulses having a duration as short as few ns, which is lesser than 10^{-6} times of the displaying time.

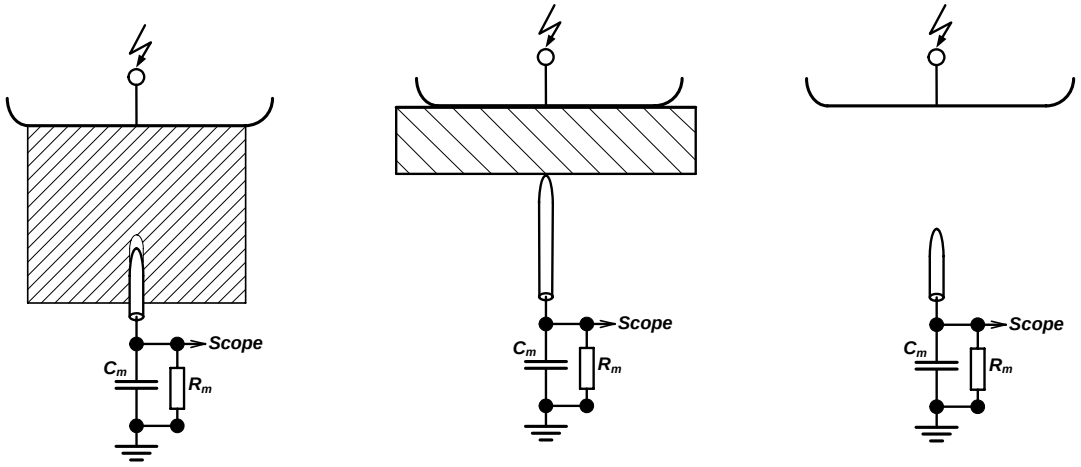

a) internal discharges in gas-filled cavities

b) internal or external discharges along surfaces

c) external discharges in ambient air

Fig. 8: Models used for measuring the PD pulse charge

For the previous considered needle-plane models the pulse charge can simply be measured if the resistor R_m originally used for measuring the shape of PD current pulses (see figures 3 to 5) is increased essentially and an additional measuring capacitor C_m is connected in parallel to R_m, as illustrated in Fig. 8. In order to avoid a superposition of subsequent appearing PD pulses, C_m must be discharged by R_m before the next PD event appears. For this parallel connection the discharging time constant is given by:

$$\tau_m = R_m * C_m \qquad (2)$$

For the here utilized circuit elements $R_m = 10\ k\Omega$ and $C_m = 1\ nF$ the discharging time constant is τ_m = 10 µs. Superposition phenomena can be avoided for PD pulse sequences having a distance greater than about $3 * \tau_m$ = 30 µs, which is equivalent to a maximum pulse repetition rate of 30 kHz. In Fig. 9 typical PD signatures are displayed for the here considered case using the classical needle-plane models presented in Fig. 8.

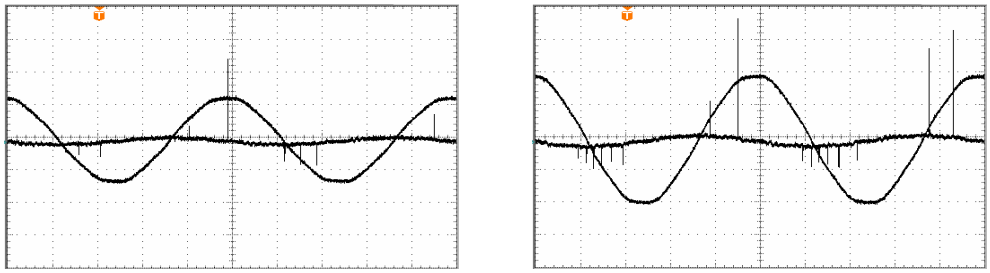

charge: 20 pC/div, time: 4 ms/div charge: 20 pC/div, time: 4 ms/div

a) cavity discharges in XLPE

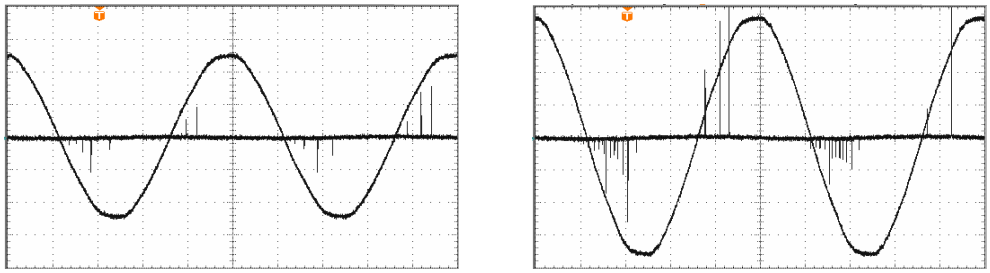

charge: 100 pC/div, time: 4 ms/div charge: 100 pC/div, time: 4 ms/div

b) gliding discharges along the surface of a solid dielectric (Toepler´s arrangement)

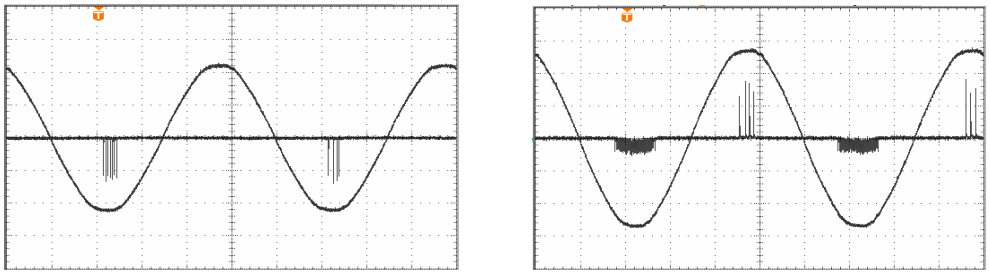

charge: 50 pC/div, time: 4 ms/div charge: 200 pC/div, time: 4 ms/div

c) corona discharges in a needle plane gap in ambient air

Fig. 9: Phase-resolved PD signatures of different discharge models close to the inception voltage (left) and substantially above the inception voltage (right)

The PD signatures displayed in Fig. 9 can be described as follows:

1. Internal discharges in gas-filled cavities

The PD pulse sequences appear in the negative half-cycle at falling test voltage and in the positive half-cycle at rising test voltage. After the negative and positive peaks of the test voltage the PD events disappear suddenly. At inception voltage the pulses occur simultaneously in both, the negative and positive half-cycle. If the test voltage is further increased the pulse magnitudes remain more or less constant, whereas the pulse repetition rate increases significantly. The charge magnitudes of the pulses sequences in both half-cycles scatter over a wide range. This is caused by the different inception voltages for positive and negative discharges as well as by the impact of the space charge accumulated in the cavity. Furthermore, the individual pulse magnitudes may scatter over a wide range even if the test voltage level remains constant. After longer stressing time it may happen that the PD events disappear finally. This is likely caused by an enhancement of the gas pressure in the cavity due to the creation of by-products. Additionally, the formation of conducting surfaces may also contribute to this appearance.

2. External discharges along surfaces in ambient air

The PD signatures of such PD events, often referred to as Toepler discharges, are qualitatively comparable to those of internal discharges, i.e. the PD events appear in the negative half-cycle at falling test voltage and in the positive half-cycle at rising test voltage, respectively. The pulse sequences disappear suddenly after the peaks of the negative and positive half cycle are reached. Furthermore, the PD events occur simultaneously in both half-cycles after the PD inception voltage is exceeded. Also the magnitudes of the negative and positive pulses are very different and may scatter for each PD pulse sequence over a wide range, even if the test voltage level remains constant. Different to internal discharges, however, the pulse magnitudes may increase excessively at rising test voltage, whereas the pulse repetition rate changes only slightly.

3. External discharges in ambient air

The PD signatures of external discharges in ambient air, often referred to as corona discharges, differ significantly from those of internal and surface discharges. So at inception voltage the PD events do not appear in both half-cycles simultaneously. First characteristic PD pulse sequences, known as Trichel pulses, are ignited in that half-cycle where the needle polarity is negative. In the other half-cycle PD events are ignited after the test voltage level is increased substantially. Independent from the polarity of the applied AC test voltage, the characteristic pulse sequences cover always the peak region, which is different to the behaviour of internal discharges and surface discharges, where the PD sequences occur at either rising or falling test voltage. In this context it should be noted, that the shape and magnitude of Trichel pulses appear well reproducible, as also evident from Fig. 9c and Fig. 10. Therefore this kind of discharges is frequently used for a functional check of the complete PD measuring circuit before starting actual PD tests.

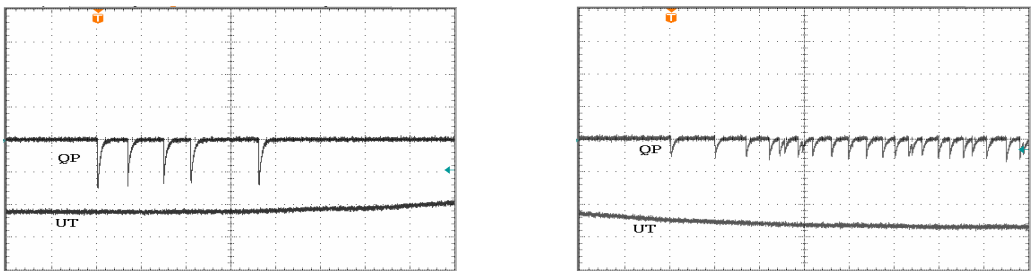

charge: 50 pC/div, time: 0.2 ms / div charge: 200 pC/div, time: 0.2 ms/div

Fig. 10: Trichel pulses near PD inception voltage (left) and substantially above inception voltage (right)

4 PD QUANTITIES

In order to increase the information on PD events the standard IEC 60270 [9] recommends besides the measurement of the apparent charge the evaluation of additional PD quantities, which are either related to the apparent charge or which are derived from the apparent charge, as well.

Apparent Charge

As mentioned already, the original PD current pulses occurring in HV apparatus cannot be measured directly because the PD source is not accessible. Consequently, only the transient voltage drop appearing across the test object terminations is detected. For an assessment of the detectable pulse charge often the approach of Gemant and Philippoff [38] is utilized, which was published already in 1932. Due to the characteristic capacitances $C_a - C_b - C_c$ illustrated in Fig. 11 this approach is often referred to as a-b-c model.

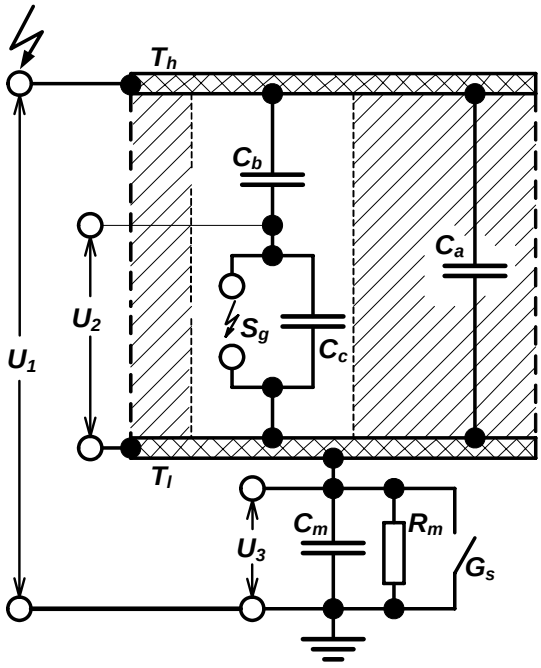

C_a – virtual test object capacitance
C_b – stray capacitance of the PD source
C_c – internal capacitance of the PD source
C_m – measuring capacitor
R_m – measuring resistor
G_s – grounding switch
S_g – spark gap
T_h – high voltage terminal of the test object
T_l – low voltage terminal of the test object
U_1 – test voltage applied
U_2 – voltage drop across the PD source
U_3 – voltage drop across R_m

Fig. 11: Equivalent circuit for evaluation the apparent charge

To symbolize the reduced voltage strength of the PD source, the capacitance C_c is bridged by a spark gap S_g having a comparatively low breakdown voltage. Records of the voltages $U_1 - U_2 - U_3$, which are representative for the a-b-c model, are shown in Fig. 12.

Here are:

U_1 – the AC test voltage across C_a applied to the test object terminals
U_2 – the partial voltage across C_c and S_g, where the grounding switch G_s is closed
U_3 – the voltage drop across C_m and R_m, where the grounding switch G_s is opened

Let us first consider the partial voltage drop across the PD defect designated as U_2, where the grounding switch G_s is closed. Under this condition U_2 is characterized by subsequent voltage jumps, which appear only at falling and rising test voltage U_1. As expected, at higher magnitude of U_1 the repetition rate of the voltage jumps U_2 is increased substantially whereas the magnitudes remain more or less constant.

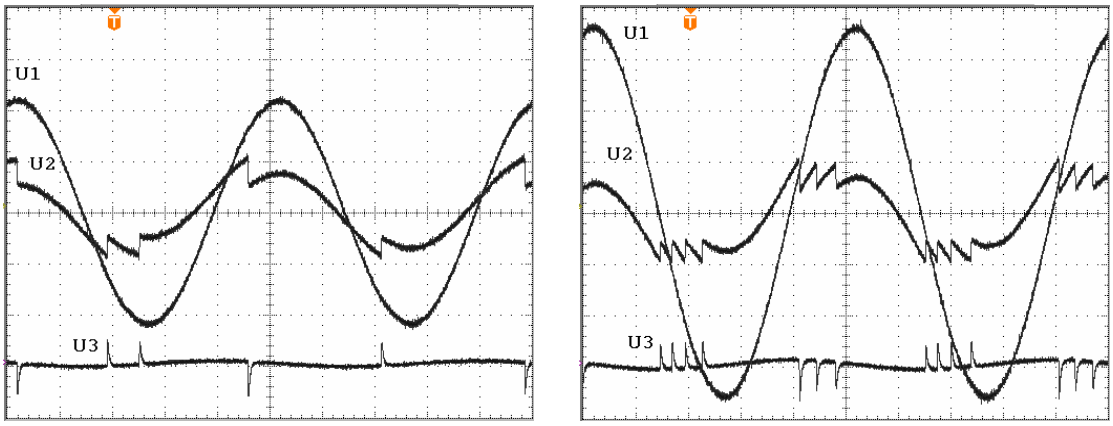

a) U1 near the PD inception voltage b) U1 substantially above the PD inception voltage

Fig. 12: Characteristic voltages recorded for the equivalent circuit according to Fig. 11

If the grounding switch G_s is now opened, voltage pulses across the measuring impedance designated as U_3. Here the measuring impedance is composed of the parallel connection of the measuring capacitor C_m and the measuring resistor R_m, where the time constant of the measuring circuit is given by:

$$\tau_m = R_m * C_m \qquad (3)$$

If the value of τ_m is significantly larger than the duration of the pulse charge transfer, which is usually below the µs range, the impact of R_m on the pulse magnitude can be neglected. Thus the transient voltage U_3, which appears temporarily across C_m, is proportional to those appearing across the virtual test object capacitance C_a designated as U_1. Because the series connection of C_a and C_m forms a voltage divider, see Fig. 11, it can be written:

$$U_3 = U_1 * C_a / (C_a + C_m) \qquad (4)$$

For the condition $C_m >> C_a$ follows the following simplification:

$$U_3 * C_m = U_1 * C_a = q_a \qquad (5)$$

That means the charge q_a stored temporarily in the virtual test object capacitance C_a can be evaluated quantitatively by measuring the transient voltage magnitude U_3 across the measuring capacitance C_m. For the here considered example according to Fig. 11 a value of C_m = 1 nF was used and U_3 was about 50 mV. Therefore, the pulse charge magnitude can be assessed as about 50 pC.

Due to the always satisfied condition $C_b << C_a$ the measurable charge can also be expressed by:

$$q_a = U_1 * C_a = U_2 * C_b \qquad (6)$$

If this equation is multiplied by the ratio $C_a / C_a = 1$ follows finally:

$$q_a = U_2 * C_a * C_b / C_a = q_c * C_b / C_a \qquad (7)$$

That means that the charge q_a measurable at the test object terminals is only a small fraction of the true charge q_c created at the PD site. This is because of the extremely small stray capacitance C_b of the PD defect compared to that of the test object C_a, i.e. $C_b / C_a << 1$.

In this context it seems also important to note that the apparent charge q_a is indirect proportional to the virtual test object capacitance C_a, see equation (7). Therefore, for a given value of the true charge q_c the magnitude of the measurable apparent charge q_a is reduced if the test object capacitance, C_a, is increased. That means, the apparent charge is not a direct measure of the PD intensity and thus not the only criterion for an assessment of the insulation condition of HV apparatus.

Related and derived PD quantities

Quantities related to the test voltage

PD test voltage

Specified AC test voltage magnitude applied for a specified PD test procedure during which PD events exceeding a specified apparent charge magnitude should not occur in the test object.

PD inception voltage U_i

Applied AC voltage magnitude at which repetitive occurring PD pulses exceed a specified apparent charge magnitude when the voltage applied to the test object is gradually increased from a level at which no PD events occur, which exceed the specified partial discharge magnitude.

PD extinction voltage U_e

Applied AC voltage magnitude at which PD pulses of a specified apparent charge magnitude disappear when the voltage applied to the test object is gradually decreased from a level at which PD events occur, which exceed a specified partial discharge magnitude.

Quantities derived from the PD recurrence

Pulse repetition rate n

Total number N_x of PD pulses occurring within a chosen reference time interval T_0 divided by this reference time interval:

$$n = N_x / T_0 \qquad (8)$$

For measuring n, the connection of an oscilloscope or of a suitable counter to the output of the PD measuring instrument is recommended. For PD instruments with bi-directional or oscillatory response a pulse shaping is required to get only one count per pulse. To resolve the maximum pulse repetition rate the counter applied should have a sufficiently short pulse resolution time

Pulse repetition frequency N

Total number N_y of equidistant appearing calibrating pulses occurring within a chosen reference time interval T_r divided by this reference time interval:

$$N = N_y / T_r \qquad (9)$$

Phase angle Φ_i

Time difference Δt_i between the negative-to-positive crossing of the applied AC test voltage and the considered PD pulse multiplied with 360^0 and divided by the duration T_c of one cycle of the AC test voltage:

$$\Phi_i = (360^0) * \Delta t_i / T_c \qquad (10)$$

The phase angle is expressed in degrees.

Average discharge current I

Accumulated absolute values of the apparent charge of subsequent appearing PD pulses within a chosen reference time interval T_r divided by this reference time interval:

$$I = (/q_1/+/q_2/+...+/q_i/) / T_r \qquad (11)$$

The average discharge current is expressed either in Coulombs per second (C/s) or in Amperes (A). It has to be taken care that measuring errors may be caused by:

- amplifier saturation due to high pulse repetition rate
- pulses occurring at separation time less than the pulse resolution time of the PD instrument
- apparent charge magnitudes occurring below the detection threshold level of the PD instrument

Discharge power P

Average power of a PD pulse sequence fed into the termination of the test object within a chosen reference time interval T_r divided by this reference time interval:

$$P = (q_1 * u_1 + q_2 * u_2 + ... + q_i * u_i) / T_r \qquad (12)$$

Here are $u_1, u_2, ...u_i$ the instantaneous values of the applied AC test voltage at the time of occurrence ($t_1, t_2, ...t_i$) of individual PD pulses having the apparent charge magnitudes $q_1, q_2, ...q_i$. The discharge power is expressed in Watts per recording time (W / T_r).

From a physical point-of-view the discharge power seems more informative than the apparent charge for an assessment of the PD severity. However, it has to be taken care that a measurement of the discharge power at acceptable accuracy requires an extremely high dynamic range, because PD pulses of very low apparent charge magnitudes but high pulse repetition rate may create a discharge power similar to pulses of very high apparent charge magnitude but low repetition rate. According to practical experience a dynamic range as high as 1000 : 1 seems required for measuring both, the apparent charge magnitude and the pulse repetition rate. That means, if the apparent charge magnitudes range, for instance, between 10 pC and 10000 pC and the pulse repetition rate ranges between 100 Hz and 100 kHz, these parameters should be evaluated at sufficient low measuring uncertainty without changing the settings of the PD measuring facility, which can not be achieved for commercially available PD instruments.

Quadratic rate D

Accumulated values of the squares of the apparent charge of subsequent PD pulses appearing within a chosen reference time interval T_r divided by this reference time interval:

$$D = [(q_1)^2+(q_2)^2+...+(q_i)^2\ ] / T_r \qquad (13)$$

The quadratic rate is expressed in (Coulombs)^2 per second (C^2/s). It has to be taken care that fatal measuring errors may occur due to to a limited measuring dynamic as discussed above for the PD quantity discharge power.

Finally it should be noted, that quality assurance PD tests of HV apparatus after manufacturing are based mainly on the PD quantity apparent charge as well as on the PD inception and extinction voltage.

5 PD MEASURING CIRCUIT

Coupling Modes

To ensure reproducible and well comparable test results the PD measuring circuit is specified in IEC 60270 [9] accordingly, where three basic PD test circuits are recommended which differ by the arrangement of the measuring impedance Z_m. In Fig. 13a the measuring impedance Z_m is connected in series with the coupling capacitor C_k. The noise blocking filter Z_n is intended for the rejection of electromagnetic noises coming from the HV side of the test transformer T_r. Moreover it prevents a short cut for the PD signal through the HV test transformer. It has to be taken care that the HV leads are designed PD-free and the grounding leads are kept as short as possible in order to minimize the inductance and thus the impact of electromagnetic interferences on the PD test results.

The PD detection sensitivity can substantially be increased if Z_m is connected in series with the grounding of the test object, as shown in Fig. 13b. Here the return path for the high frequency PD transients is formed by the coupling capacitor C_k. This circuit, however, requires an interruption of the ground connection of the HV apparatus under test, which can be done in practice only in special cases. Furthermore it has to be taken into account, that the AC current flowing through the test object is also passing Z_m. Because this magnitude could become extremely high it may damage Z_m, in particular in case of an unexpected breakdown of the test object.

External electromagnetic noises disturbing sensitive PD measurements can be eliminated at certain extend if a balanced bridge is employed, as illustrated in Fig. 13c. Here both, the measuring and reference branch, are composed similar to Fig. 13b, i.e. a separate coupling capacitor C_k is not utilized. Adjusting the impedances of Z_{m1} and Z_{m2} the bridge can be balanced accordingly and the common mode external noises are rejected effectively by means of the differential amplifier, which is often part of the input unit of the PD measuring

instrument M_i. Different to the common mode noise signal, PD events originated in the test object can sensitively be detected.

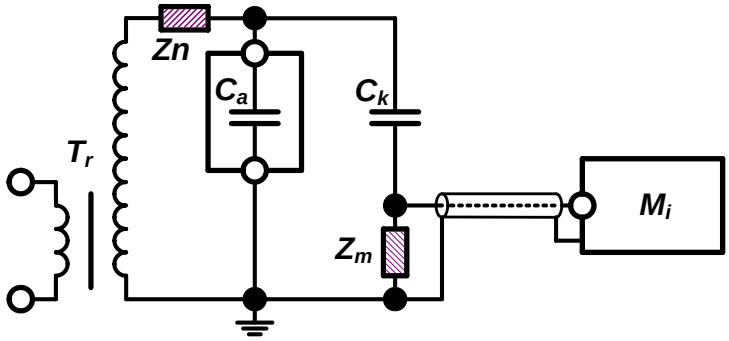

a) Measuring impedance Z_m in series with the coupling capacitor C_k

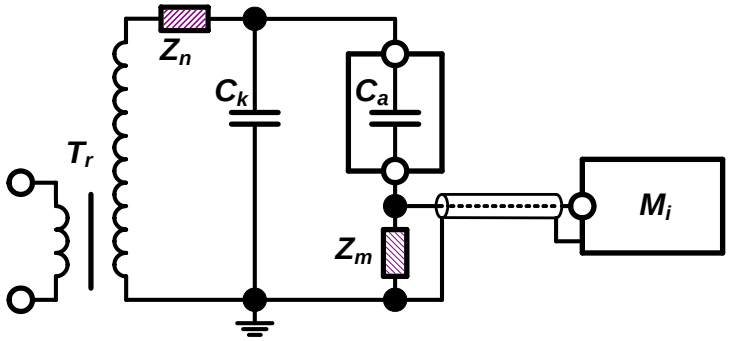

b) Measuring impedance Z_m in series with the test object capacitor C_a

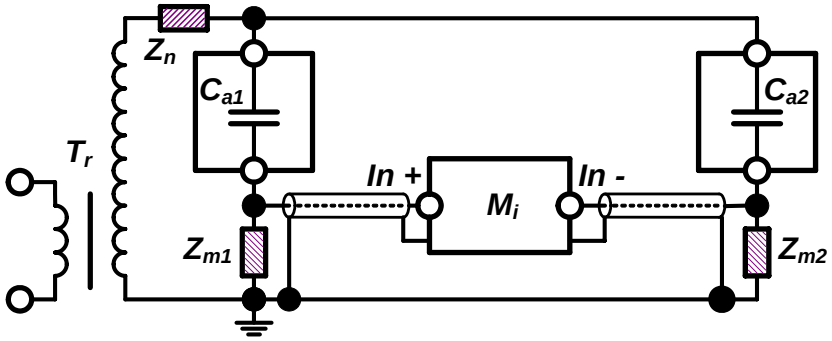

c) Balanced bridge using a reference branch *(C_{a2}, Z_{m2})* in parallel to the test branch *(C_{a21}, Z_{m1})*

T_r – HV test transformer
Z_n – Noise blocking filter
C_a – Virtual test object capacitance
C_k – Coupling capacitor
Z_m – Measuring impedance as part of the coupling device
M_i – PD measuring instrument

Fig. 13: Basic PD test circuits recommended in IEC 60270 [9]

This is, because the PD transients through C_{a1} and C_{a2} and thus passing Z_{m1} and Z_{m2} appear at opposite polarity at both, the non-inverting input (In+) and the inverting input (In-) of the differential amplifier, which is therefore be amplified and further processed. To ensure a high common mode rejection the bridge should be designed as symmetrical as possible. Thus it is advisable to use a complementary test object for the reference branch, where the parameters, such as the virtual capacitance as well as the geometrical size, should be equivalent to those of the test object. The noise rejection performance can be improved further if the differential amplifier is combined directly with both measuring impedances Z_{m1} and Z_{m2} placed inside the HV test area.

Despite of the benefits of the balanced bridge for noise suppression the most common circuit employed in practice is that where the measuring impedance Z_m is connected in series with the coupling capacitor C_k, see Fig. 13a.

An option of the PD test circuit reported in Fig. 13a is the so-called bushing tap coupling mode illustrated in Fig. 14. Here the coupling capacitor C_k is presented by the high voltage bushing capacitance C_1, and the measuring impedance Z_m as essential part of the coupling device D_c is connected to the tap of the capacitive graded bushing, usually intended for loss factor measurements. This circuit is employed advantageously for induced voltage tests of liquid-immersed power transformers.

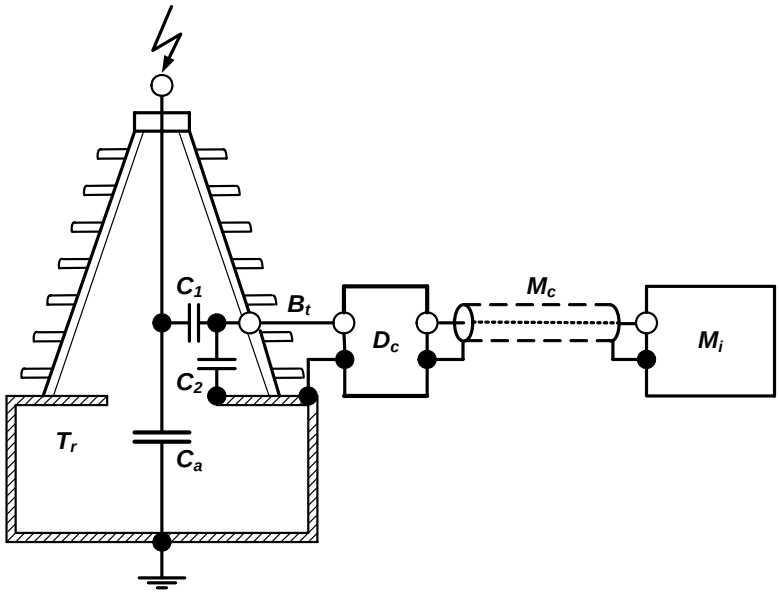

T_r – *Transformer under test*
C_a – *Virtual test object capacitance*
C_1 – *HV capacitance of the bushing*
C_2 – *LV capacitance of the bushing*
B_t – *Bushing tap*
D_c – *Coupling device*
M_c – *Measuring cable*
M_i – *Measuring instrument*

Fig. 14: Bushing tap coupling mode

The major components of common PD test circuits recommended in IEC 60270 [9] are illustrated in Fig. 15 and will now be considered more detail.

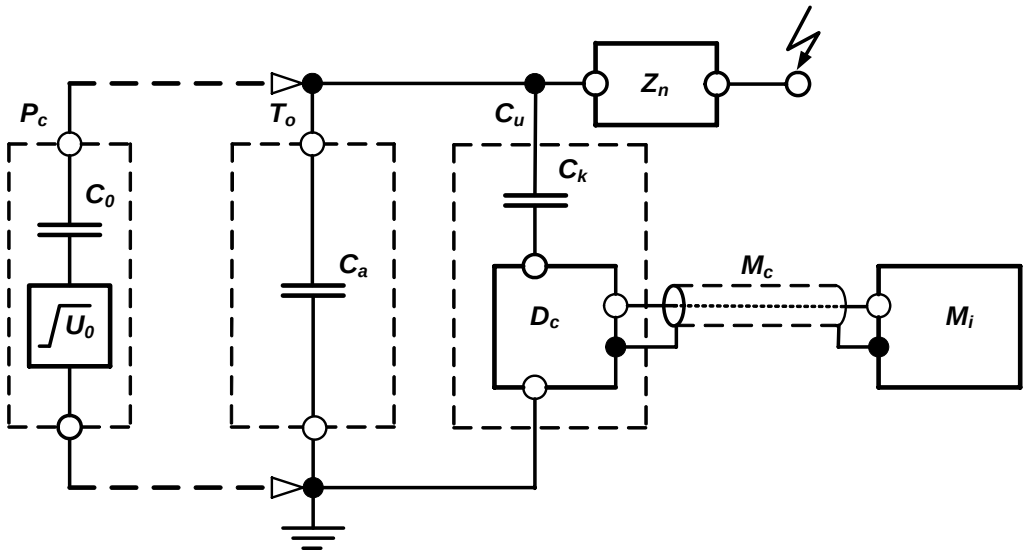

P_c – *PD calibrator*
C_0 – *Calibrating capacitor*
U_0 – *Step pulse generator*
T_o – *Test object*
C_a – *Virtual test object capacitance*
Z_n – *Noise blocking filter*
C_u – *PD coupling unit*
C_k – *Coupling capacitor*
D_c – *Coupling device*
M_c – *Measuring cable*
M_i – *PD measuring instrument*

Fig. 15: Major components of common PD measuring circuits

PD Coupling Unit

Coupling Capacitor

The coupling capacitor C_k is intended for the transfer of the high frequency spectrum of the PD signal appearing across the virtual test object capacitance C_a to the coupling device D_c. Simultaneously the test voltage is attenuated down to a harmless magnitude. The coupling capacitor C_k must be PD-free up to the highest AC test voltage level and should be of low inductance in order to transmit the high frequency PD signal without exciting disturbing oscillations. The capacitance of C_k should be chosen sufficiently high in order to minimize the impact of the stray capacitances of the measuring circuit on the reduction of the magnitudes of the PD pulses if transferred to the coupling device D_c. Moreover, the condition $C_k / C_a > 0.1$ should be satisfied to achieve a decent measuring sensitivity.

Coupling Device

The coupling device D_c forms in principle a four-terminal network, sometimes referred to as quadrupole. It is equipped with the measuring impedance Z_m as the main part which converts the input PD current pulses into equivalent output voltage pulses to be routed via a measuring cable to the PD measuring instrument M_i, see Fig. 15. Additionally the coupling device is composed with supplementary elements for signal filtering in order to eliminate disturbing harmonics caused by the AC test voltage supply. Moreover, a fast over-voltage protection unit is required for suppressing over-voltages which may result from unexpected breakdowns of the test object. To ensure an optimum PD signal transmission, the coupling device D_c should be located physically as close as possible to the coupling capacitor C_k and, for safety reasons, always inside the high voltage test area.

The series connection of the coupling capacitor C_k with the measuring impedance Z_m forms a high-pass filter, as evident from Fig. 16. This determines the lower limit frequency f_1 of the complete PD measuring circuit. If the value of f_1 is specified and L_m is initially neglected, the required value for C_k can simply be evaluated for a given value of the measuring resistor R_m.

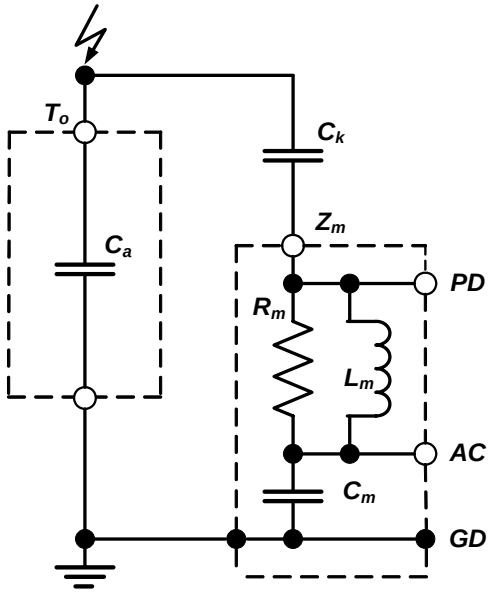

T_o – Test object	*R_m – Measuring resistor*
C_a – Virtual test object capacitance	*C_m – Measuring capacitor*
C_k – Coupling capacitor	*PD – Output PD pulses*
Z_m – Measuring impedance	*AC – Output AC test voltage*
L_m – Shunt inductor	*GD – Grounding terminal*

Fig. 16: Equivalent circuit of the PD coupling unit

For better understanding let us assume the following circuit parameters:

Resistive impedance: $R_m = 500\ \Omega$, Lower cut-off frequency: $f_1 = 100\ kHz$

Using the formula for the lower limit frequency:

$$f_l = 1 / (2\pi * C_k * R_m) \quad (14)$$

the value required for the coupling capacitor can be calculated as:

$$C_k = 1 / (2\pi * f_l * R_m) = 3.2\ nF \quad (15)$$

In this context it has to be taken care that the AC current magnitude flowing through C_k may cause a comparatively high voltage drop across R_m and could thus damage the input unit of the PD instrument. If, for instance, an exciting frequency of $f_{ac} = 400\ Hz$ is applied for an induced PD test of a power transformer, the capacitive impedance of the above calculated coupling capacitor is:

$$Z_c = 1 / (2\pi * f_{ac} * C_k) = 1 / (2\pi * 400\ Hz * 3.2\ nF) = 125\ k\Omega \quad (16)$$

Therefore the voltage divider ratio at $f_{ac} = 400\ Hz$ is given by 500 Ω / 125 kΩ = 1 / 250. Consequently, an AC test voltage magnitude of, for instance, $U_{ac} = 200\ kV$ causes a voltage drop across the resistive measuring impedance R_m as high as 200 kV / 250 = 800 V. To reduce this dangerous voltage the measuring resistor R_m is usually shunted by an inductor L_m as illustrated in Fig. 16. It has to be taken care that the lower limit frequency is not decreased substantially. This condition is accomplished by:

$$L_m > 10 * R_m / (2\pi * f_l) = L_m > 10 * R_m / (2\pi * 100\ kHz) = 8\ mH \quad (17)$$

For the previously assumed maximum test frequency of $f_{ac} = 400\ Hz$ the inductive impedance is:

$$Z_l = 2\pi * 400\ Hz * L_m = 20\ \Omega \quad (18)$$

The resulting divider ratio of the parallel connection of L_m and R_m in series with C_k, see Fig. 16, is approximately 20 Ω / 125 kΩ = 1 / 6250. That means a test voltage level of 200 kV would now cause an AC voltage magnitude of only 32 V, which can well be accepted.

In order to display the PD pulses in a phase-resolved manner, using an oscilloscope or a computer-based PD measuring system, the PD coupling unit can accordingly be configured, as also illustrated in Fig. 16. Here the low voltage arm of the capacitive divider is represented by a measuring capacitor designated as C_m. Because of the very different frequency spectrum of the PD pulses and the AC test voltage both signals appear completely separated at the outputs “PD” and “AC”. If, for instance, again a test voltage level of 200 kV is assumed, which should be attenuated down to 20 V, a divider ratio of 1: 10 000 is required. For the above calculated value of C_k = 3.2 nF this condition is satisfied for C_m = 32 µF.

6 PD MEASURING INSTRUMENTS

Analogue PD Signal Processing

Operation principle

A simplified bloc diagram of classical PD instruments using analogue pulse processing is shown in Fig. 17. To ensure an optimum pulse magnitude for signal processing the matching unit at the input is adjusted accordingly. Because a high-pass filter is formed by the series connection of C_k and Z_m shown in Fig. 16, the

PD pulses captured from the test object terminals are differentiated. Therefore, they must be integrated again to evaluate the apparent charge q_a. For this generally a band-pass-amplifier is utilized as will be discussed in more detail below.

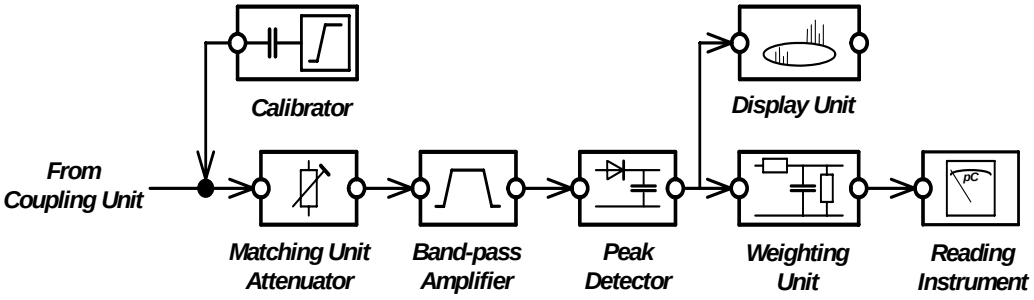

Fig. 17: Bloc diagram of an analogue PD measuring instrument

Analogue PD measuring instruments are furthermore equipped with a quasi-peak detector combined with a weighting unit and a reading instrument in order to display the "largest repeatedly occurring PD magnitude" as defined in IEC 60270 [9]. The phase resolved PD pulses are generally visualized either by a built-in oscilloscope or by an external connected display unit, such as a separate oscilloscope or a computer. This supports not only for the recognition of PD sources but also the identification and thus the elimination of disturbing noises. In order to ensure reproducible and comparable measurements both, the frequency characteristics as well as the pulse train response of PD instruments are also specified in IEC 60270 [9].

PD Pulse Response

Without going into details it can be stated that the evaluation of the apparent charge is based on the so-called quasi-integration. According to [72, 93, 94, 98, 101] this can be performed by means of a band-pass filter, which is tuned for a measuring frequency range where the amplitude frequency spectrum of the captured PD pulses is nearly constant, see Fig. 18.

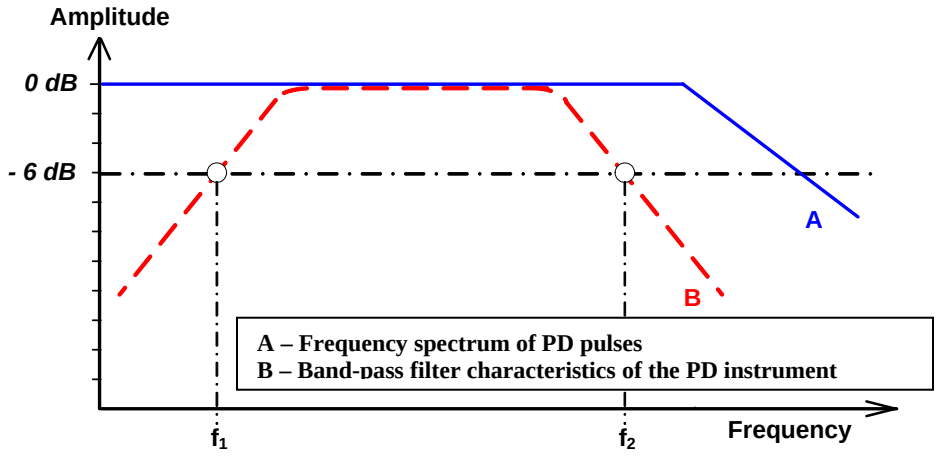

Fig. 18: Principle of the quasi-integration of PD pulses

Under this condition the response of the band-pass filter is characterized by an output voltage pulse which peak value is proportional to the input current -time signal representing the apparent charge. It should be noted that the duration of the output pulse is much longer than those of the input PD pulse. Under practical condition the requirement for a quasi-integration of PD pulses is satisfied if the maximum measuring frequency is limited below 500 kHz, as recommended in IEC 60270 [9]. In this context it should be underlined that the quasi-integration is only governed by the upper limit frequency f_2 and not by the lower limit frequency f_1. Depending on the band-width $\Delta f = f_2 - f_1$ PD measuring instruments are classified according to IEC 60270 [9] as wide-band and narrow band instruments, as will be discussed now:

1. Wide-band instruments

Such types of instruments are basically equipped with a high sensitive amplifier of specified band-pass characteristics, where the lower and upper limit frequencies can be adjusted either continuously or stepwise. According to IEC 60270 [9] the following characteristic frequencies are recommended:

Lower limit frequency:	$30\ kHz < f_1 < 100\ kHz$
Upper limit frequency:	$f_2 < 500\ kHz$
Band-width:	$100\ kHz < \Delta f = f_2 - f_1 < 400\ kHz$

In this context it should be noted that the term "wide-band" has to be understood in comparison with the filter characteristics of the PD processing unit, i.e. the band-with $\Delta f = f_2 - f_1$ is equal or larger than the lower limit frequency f_1. From a physical point of view, however, only a narrow frequency band of the PD pulses is processed, because the frequency spectrum of original PD pulses covers a range up to some 100 MHz or even more[53, 61, 62 and 67].

The pulse response of PD instruments equipped with a band-pass filter is a critical damped oscillation, as displayed in Fig. 19, where the duration of the output pulse is substantially larger than that of the input PD pulse. Due to this performance the resolution time for consecutive PD pulses is in the order of tens of µs which is equivalent to a pulse repetition rate below 100 kHz. Even if the shape parameters of the output pulses are strongly different from those of the input pulses, the PD pulse polarity can be identified in most cases, which is helpful for the identification of the PD sources.

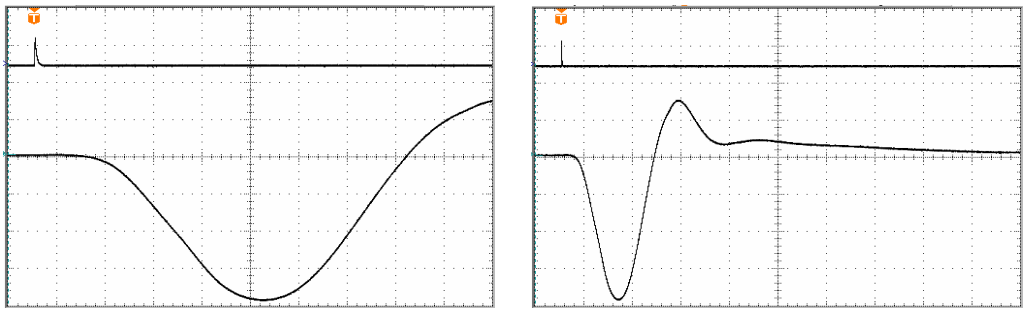

time base: 1 µs/div — time base: 4 µs/div

upper trace – input pulse — lower trace – output signal

Fig. 19: PD pulse response of a conventional wide-band PD instrument

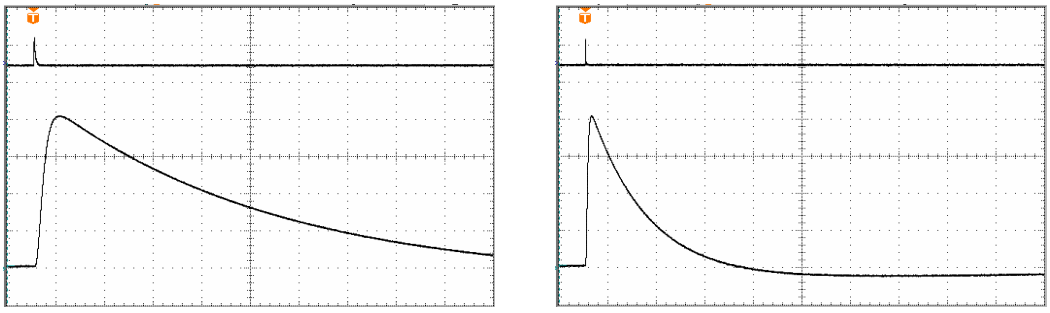

time base: 1 µs/div time base: 4 µs/div
upper trace – input pulse lower trace – output signal

Fig. 20: PD pulse response of a wide-band PD instrument equipped with an electronic integrator

It should be noted that the required integration of the input PD pulses can be performed not only by amplifiers having a suitable band-pass filter characteristic as presented above, but also by means of an active integrator [77, 86, 101], as shown in Fig. 20. The pulse response of such an integrator is displayed more in detail in Fig. 21which reveals, that the output pulse magnitude is proportional to the area of the input signal and is thus a measure for the apparent charge. The pulse resolution time of active integrators designed for PD pulse processing is usually less than 10 µs which is equivalent to a pulse repetition rate above 100 kHz [101].

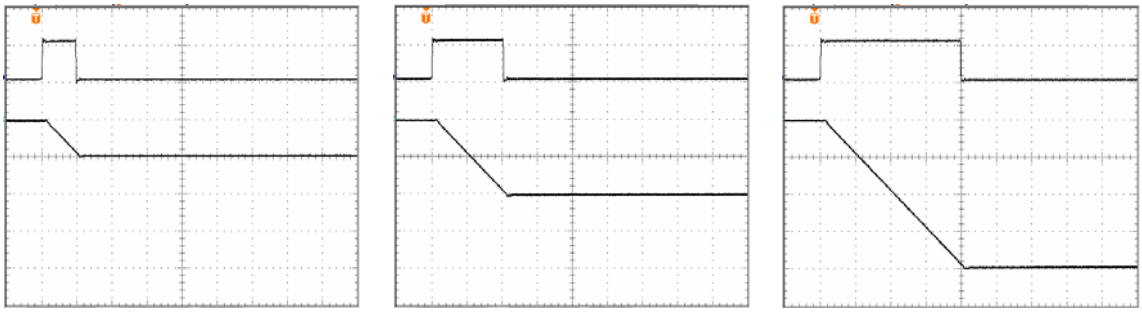

a) pulse duration: 100 ns b) pulse duration: 200 ns c) pulse duration: 400 ns
uper trace – input rectangular pulse lower trace – output signal time base: 100 ns/div

Fig. 21: Rectangular pulse response of an electronic integrator

2. Narrow-band instruments

Such types of instruments are basically equipped with a high sensitive narrow-band amplifier. The mid-band frequency f_m can be tuned continuously whereas the band-width Δf is either fixed or stepwise selectable. In IEC 60270 [9] the following characteristic measuring frequency ranges are recommended:

Mid-band frequency: $50\ kHz < f_m < 1000\ kHz$
Band-width: $9\ kHz < \Delta f < 30\ kHz$

From these frequency parameters follows that the bandwidth is essentially lower than the mid-band frequency, which is used in IEC 60270 for the classification of narrow-band instruments. The pulse response

of such instruments is characterized by a slightly damped oscillation as evident from Fig. 22. Here the maximum magnitude of the envelope of the output signal is proportional to the apparent charge of the input signal. Such narrow-band devices are often used together with a coupling unit providing a resonance frequency f_0, where the mid-band frequency f_m of the PD instrument is fixed at f_0.

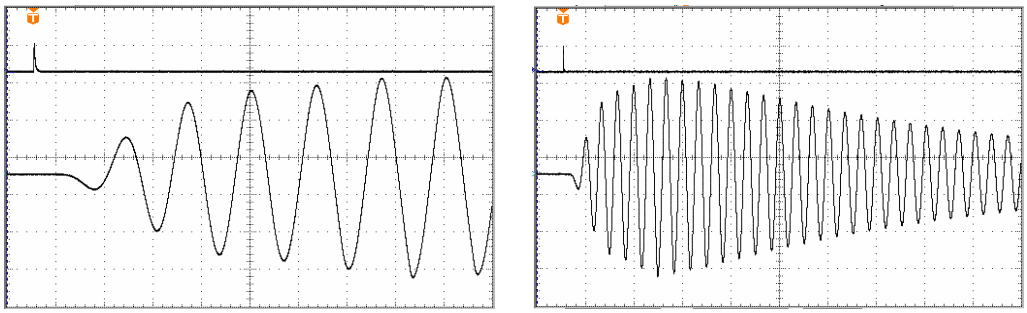

time base: 1 µs/div upper trace – input pulse

time base: 4 µs/div lower trace – output signal

Fig. 22: PD pulse response of a narrow-band PD instrument

One main back draw of narrow-band instruments is the pure resolution time for subsequent PD pulses, which is in the order of some 100 µs due to the slightly damped oscillation. This corresponds to a pulse repetition frequency of about 10 kHz, which is 10 times lower than those of wide-band instruments. This long oscillation may also cause erroneous measurements not only at a PD pulse repetition rate above 10 kHz but even if reflected or oscillating pulses are excited, due to travelling wave phenomena in long power cables and the propagation of PD pulses in the windings of power transformers and rotating machines. Another disadvantage of narrow-band instruments is that the PD pulse polarity cannot be identified. The main advantage of such instrumentation is, however, that disturbing noises from radio broadcast stations can effectively be rejected by tuning the mid-band frequency accordingly.

As mentioned already, the first industrial PD tests have been performed already in the 1940´s based on the publication NEMA 107 [1 and 2]. The aim of such HV tests was to determine the radio interference voltage (RIV) which may disturb radio receivers due to PD events radiated from of HV apparatus. For this reason the radio receiver principle is utilized where the measuring frequency is tuneable in the broadcast frequency range, i.e. between 150 kHz and 30 MHz [3 and 4], and the scale of the reading instrument is calibrated in µV. A conversation factor between the apparent charge measured in pC and the RIV level measured in µV, however, exists only if the HV test voltage level is chosen close to the PD inception voltage, where the pulse repetition rate is rather small, and no any signal reflection or oscillations appear. Under this condition a RIV value of 1 µV is equivalent to an apparent charge magnitude of about 3 pC for a input impedance of the RIV meter of $Z_m = 60\ \Omega$ and PD pulse repetition rate of $N = 100\ s^{-1}$ [5, 6, 81, 90, 130].

Pulse Train Response

The magnitudes of consecutive PD pulses may scatter over a wide range, as exemplarily displayed in Fig. 23. This represents a snapshot of PD pulse sequences occurring within one cycle of the applied power frequency (50 Hz) test voltage, i.e. the recording time is 20 ms. Here pulse magnitudes between 20 and 600 pC can be observed. Another characteristic example is shown in Fig. 24, where the graphs refer to a measuring interval of 120 seconds. Here all PD pulses occurring within all 6000 cycles of the 50 Hz test voltage are superimposed. The phase-resolved PD pattern according to Fig. 24a reveals that the PD magnitudes range between about 20 pC and almost 1000 pC. The random occurrence of the apparent charge pulses is also

evident from Fig. 24b where all peaks of the captured PD pulses were recorded. Here the apparent charge ranges between about 200 pC and almost 1000 pC.

From the chosen measuring examples reported in Fig. 24 it can be concluded that the large scattering effect of the PD magnitudes seems not feasible for reproducible PD measurements and thus the specification of critical apparent charge values in the relevant HV apparatus standards. To overcome this crucial problem the measurement of the "largest repeatedly occurring PD magnitude" is recommended in IEC 60270 [9]. This is accomplished if the heavily scattering apparent charge magnitudes are averaged. Therefore the pulse train response of the quasi-peak detector as part of the PD instrument is specified according to Fig. 25. The tolerance band between the maximum and minimum reading can well be fitted if the following time constants are chosen for the quasi-peak detector:

Charging time constant: $\tau_1 < 1$ ms Discharging time constant: $\tau_2 = 440$ ms.

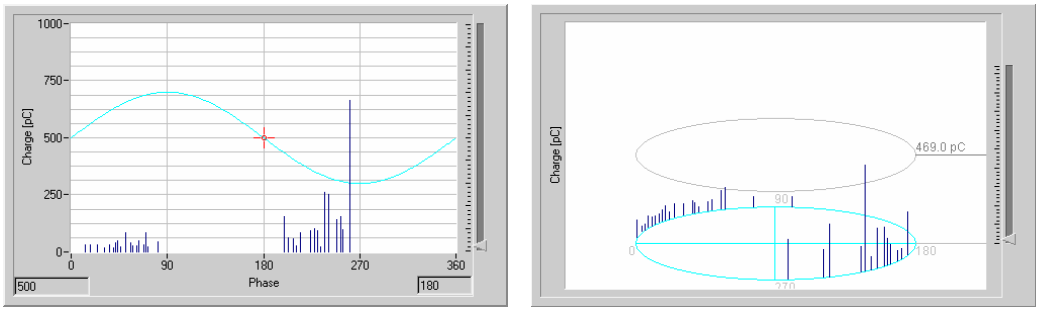

a) linear time base b) elliptical time base

Fig. 23: Snapshot of a PD pulse sequence covering one cycle of the AC test voltage (20 ms)

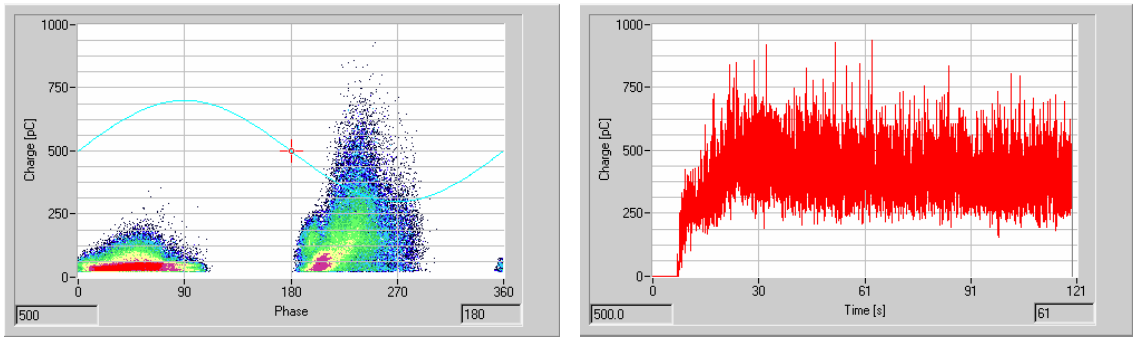

a) Phase-resolved PD pattern b) Peak-values of all captured PD pulses

Fig. 24: Random distribution of PD pulse magnitudes during a recording time of 120 seconds

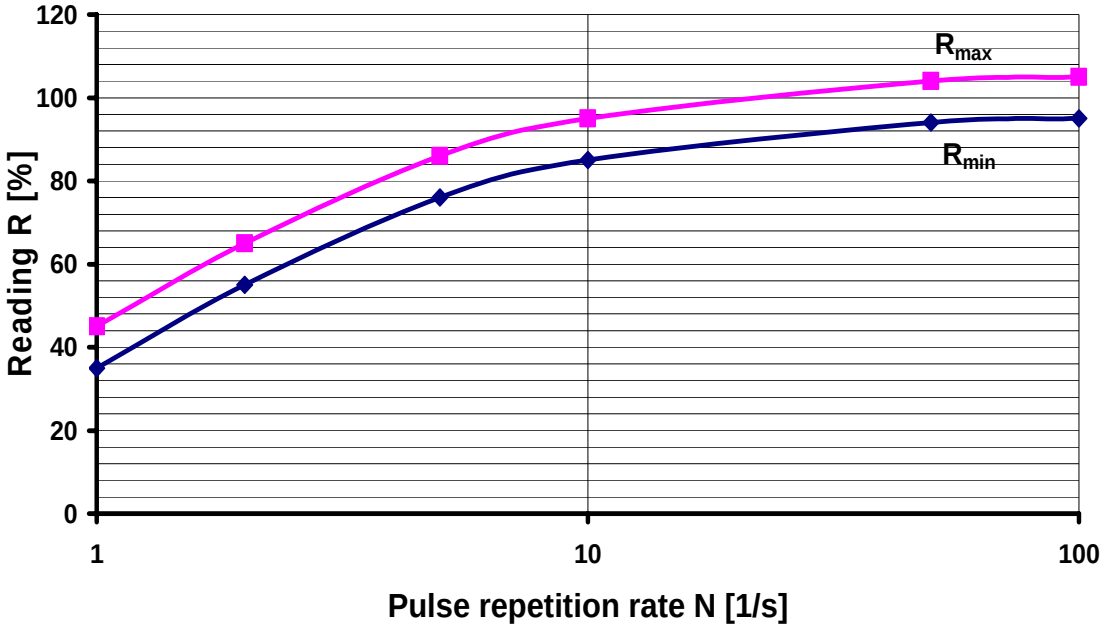

Fig. 25: Tolerance band of the PD pulse train response specified in IEC 60270 [9]

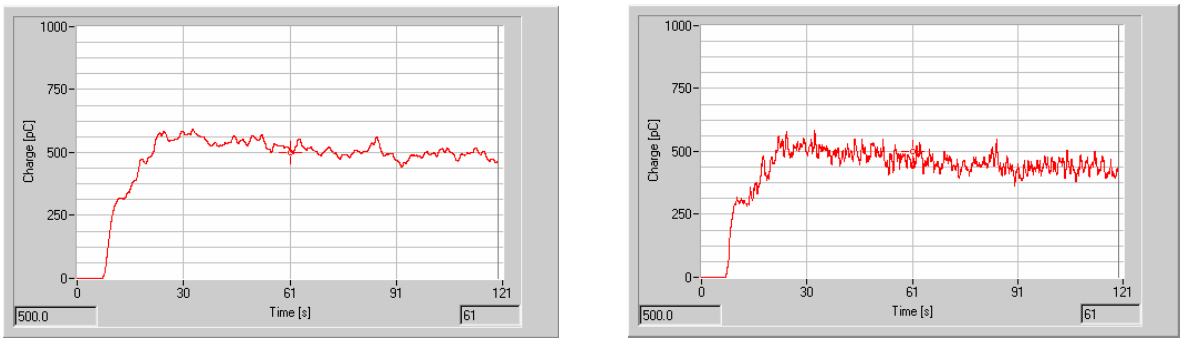

a) IEC 60270 (τ_1= 1 ms, τ_2 = 440 ms)

b) CISPR 16-1 (τ_1= 1 ms, τ_2 = 160 ms)

Note: The origin PD data are equivalent to those displayed in Fig. 24

Fig. 26: Apparent charge level of stochastically scattering PD pulses evaluated in compliance to IEC 60270 [9] and CISPR 16-1 [4]

Digital PD Signal Processing

Operation principle

For computerized PD measuring systems currently two basic measuring principles are employed, as schematically illustrated in Fig. 27. The first one shown in Fig. 27a is based on an analogue pre-processing of the PD pulses in order to create the apparent charge pulses, followed by a digital post-processing for the visualization and evaluation of the apparent charge pulses and derived PD quantities. That means the PD pulses captured from the test object are first quasi-integrated in an analogue manner using a band-pass filter, as described already. After that an A/D conversion is performed for both signals, the apparent charge magnitude of each PD event and the test voltage at the instant time of PD occurrence, followed by units for digital PD data acquisition and displaying the phase-resolved PD pulses. Additionally, the significant parameters of each PD event can be stored in the computer memory for further post-processing as well as for the visualization of phase-resolved PD patterns using the replay mode, which is comparable to the video-recorder technology [203, 204].

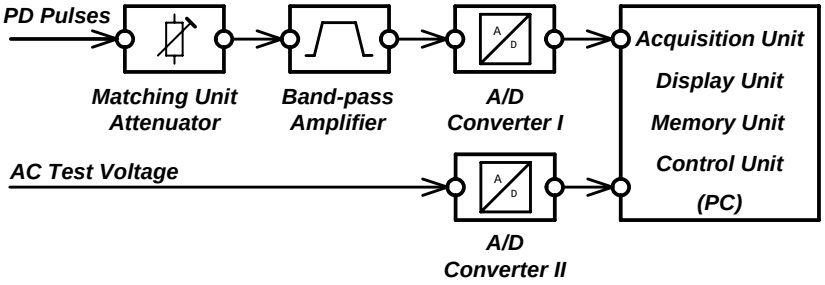

a) analogue pre-processing and digital post-processing of PD pulses

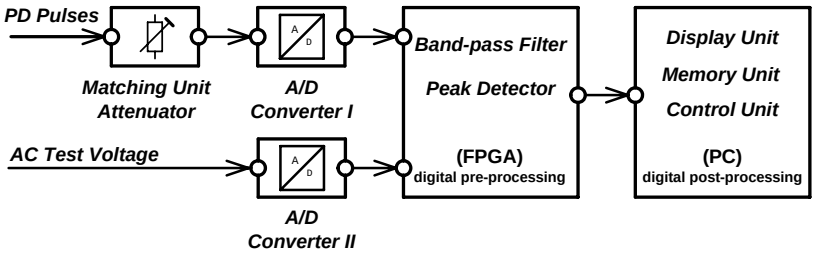

b) digital pre- and post-processing of PD pulses

Fig. 27: Bloc diagram of digital PD measuring instruments

Nowadays extremely fast analogue-digital-converters are available. Therefore the digitalization of the input PD pulses captured from the test object can be done in the real-time mode, i.e. without an analogue pre-processing as reported above. That means, the band-pass filtering required for the quasi-integration, as well as the peak detection are performed after the A/D conversion using a FPGA, see Fig. 27b. This concept extends essentially the capabilities for pulse waveform analysis used for recognition of different PD sources in HV apparatus as well as for de-noising the PD signal as reported, for instance, in [134 - 180].

The main feature of digital PD measuring instruments is the ability to store the following characteristic parameters of each PD event:

t_i – instant time of PD occurrence
q_i – apparent charge at t_i
u_i – test voltage magnitude at t_i
ψ_i – phase angle at t_i

This ensures not only an evaluation of all PD quantities as recommended in IEC 60270 [9] and summarized in Fig. 28, but also an in-depth analysis of the very complex PD occurrence.

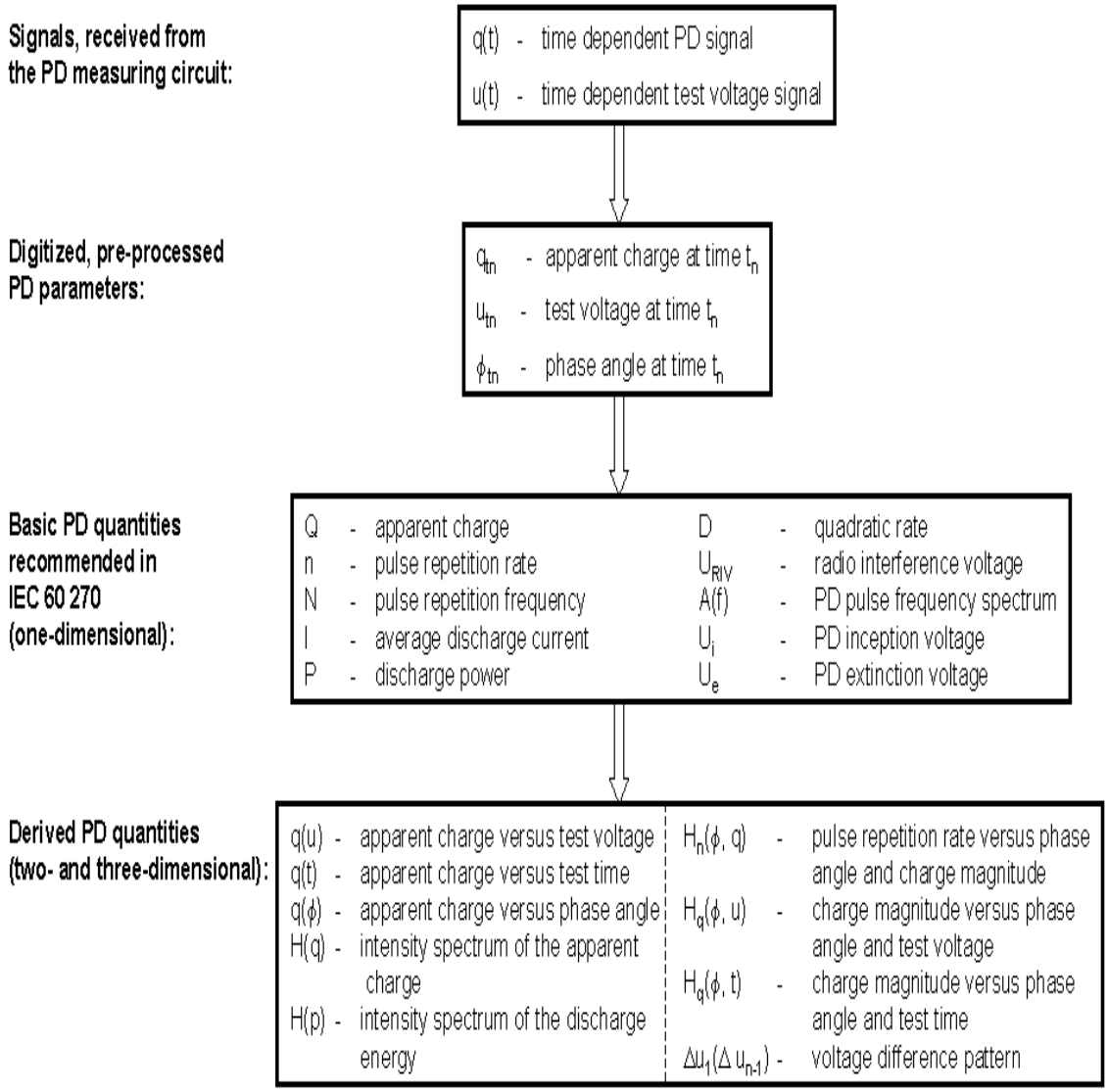

Fig. 28: PD quantities evaluated by a digital PD data acquisition [204]

Moreover digital PD measuring systems may perform the following procedures:

- Statistical analysis using phase resolved 2D and 3D pattern and pulse sequence pattern capable for classification and identification of PD sources as well as for noise rejection.

- Clustering the PD pulses in homogenous families, based on waveform analysis and spectral-amplitude diagrams in order to separate the PD pattern of different PD sources.

- Localization the PD sites using either time-domain reflectometry for power cables or multi-channel techniques for electrical machines and power transformers.

Display of PD Events

If the PD inception voltage is exceeded PD pulse trains appear usually within each cycle of the applied AC test voltage. To assess the PD activity, it was originally common practice to record the PD level versus the testing time, as illustrated in Fig. 29.

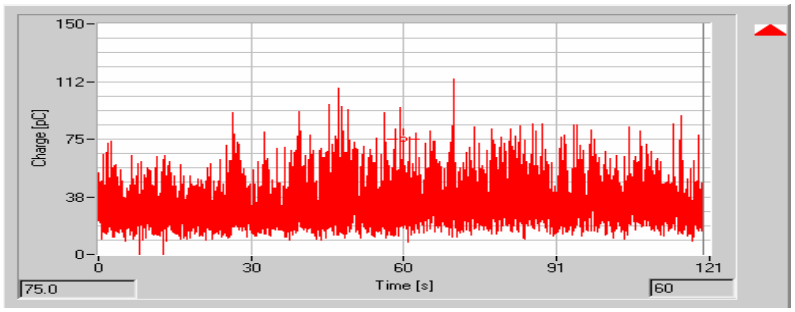

Fig. 29: Time dependent PD level measured for a power cable termination, recording time 120 seconds (6000 cycles)

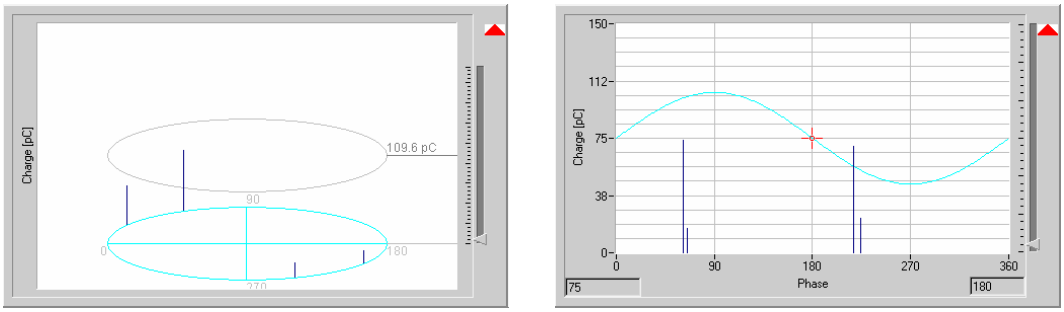

a) elliptical time base (Lissajous figure) b) linear time base

Fig. 30: Snapshot of a PD pulse sequence captured from a power cable termination appearing within an individual AC cycle (20 ms)

When the first and second edition of IEC Publication 60270 appeared [7 and 8] it was already recommended to display additionally the PD pulse trains correlated to the AC test voltage by means of cathode ray oscilloscopes (CRO). The CRO technique, however, ensures only snapshots of the phase-resolved PD pulses of individual AC cycles, as illustrated in Fig. 30.

Advanced digital PD measuring systems have improved very much not only the visualization of characteristic PD patterns but also the analysis and interpretation of PD data. As an example, Fig. 31 illustrates characteristic PD signatures obtained for a power cable termination. In Fig. 31a the 2-dimensional phase

resolved PD pattern is displayed where the recording time was 120 seconds, i.e. the peaks of the apparent charge pulses appear superimposed for 6000 subsequent AC cycles. Here the pulse repetition rate is indicated qualitatively by different colours representing the third dimension. In Fig. 31b the PD data already presented in Fig. 31a are displayed as a 3-D graph. Here the x- and y-axis represent the phase angle and the charge magnitude, respectively, whereas the z-axis refers to the pulse number. An example for the so-called PD pulse-sequence pattern [151, 153, 201, 202 and 210] is reported in Fig. 31c, which is based on the difference of the instantaneous test voltage values evaluated between two successive PD pulses. Finally, a statistical fingerprint is displayed in Fig. 31d, where the pulse number vs. the phase angle as well as the peak and mean values of the density of the pulse distribution function are evaluated, as described in [142, 144 and 148].

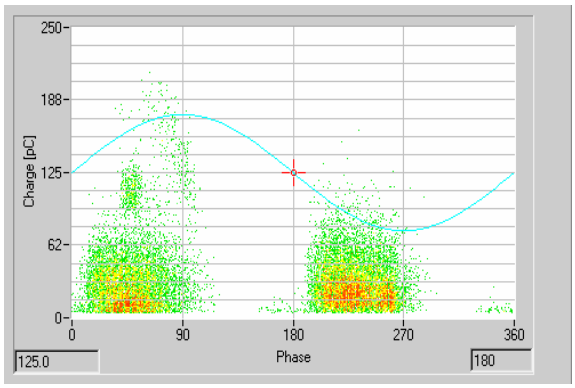

a) phase resolved PD pattern

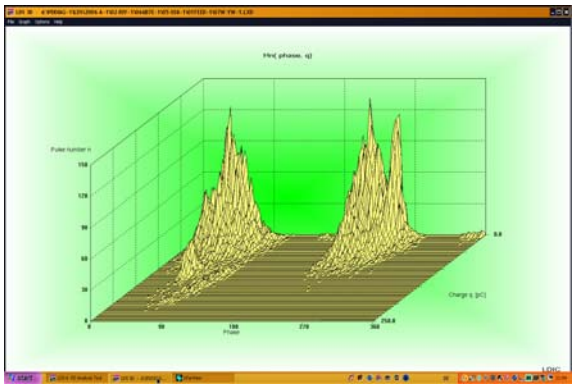

b) PD pulse number versus phase angle and charge

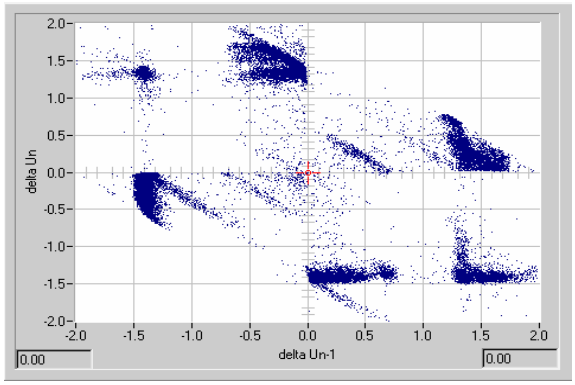

c) PD pulse-sequence pattern

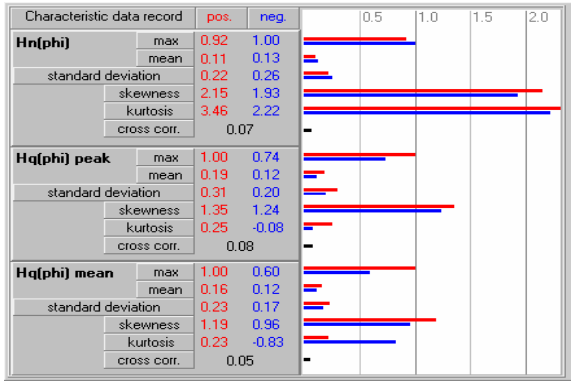

d) statistical PD fingerprint

Fig. 31: Characteristic PD signatures created for a PD source in a power cable termination recording time 120 seconds (6000 cycles)

Another measuring example is shown in Fig. 32 which refers to three-phase diagrams used for automatic cluster recognition, as reported in [205 and 212]. Nowadays powerful tools are also available for analysing the PD pattern correlated to a specific cluster. This is based on the separation of characteristic clusters obtained for different pulse shapes, which may be received for different PD sites in HV apparatus as reported, for instance, in [173, 174 and 180]. A measuring example for this is displayed in Fig. 33. Moreover, this feature may also be utilized for de-noising the PD signal because the shapes of PD pulses are generally very different from signals originated from electromagnetic noises, as also evident from Fig. 33. As the laboratory test is concerned, the use of PD monitoring systems with such advanced data processing features could be very useful for the identification of several PD sources in HV apparatus. In this context it should be noted,

however, that in case of "go/not go" tests this advantage is limited as the component standards specify critical PD limits independently of their cause.

The post-processing of PD data as well as the visualization of phase-resolved PD signatures and the evaluation of statistical PD data and even the de-noising of PD signals, however, are outside of the scope of IEC 60270 [9] and will thus not be discussed here in more detail.

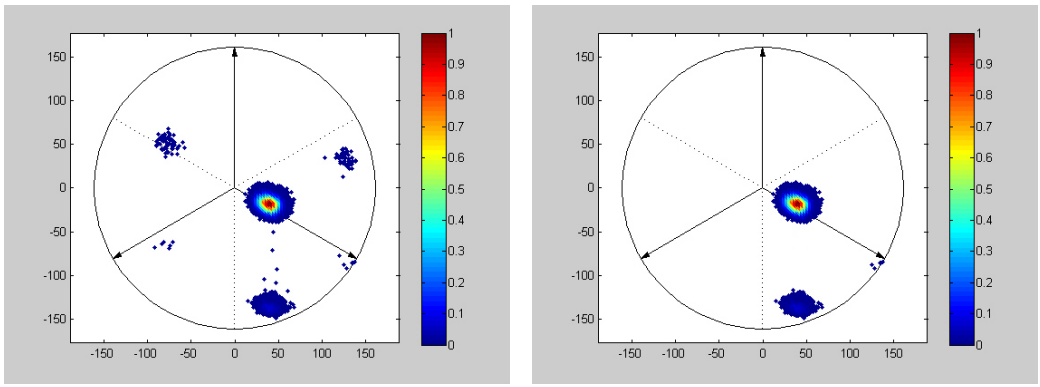

Fig. 32: Three-phase diagrams for cluster recognition according to [205]

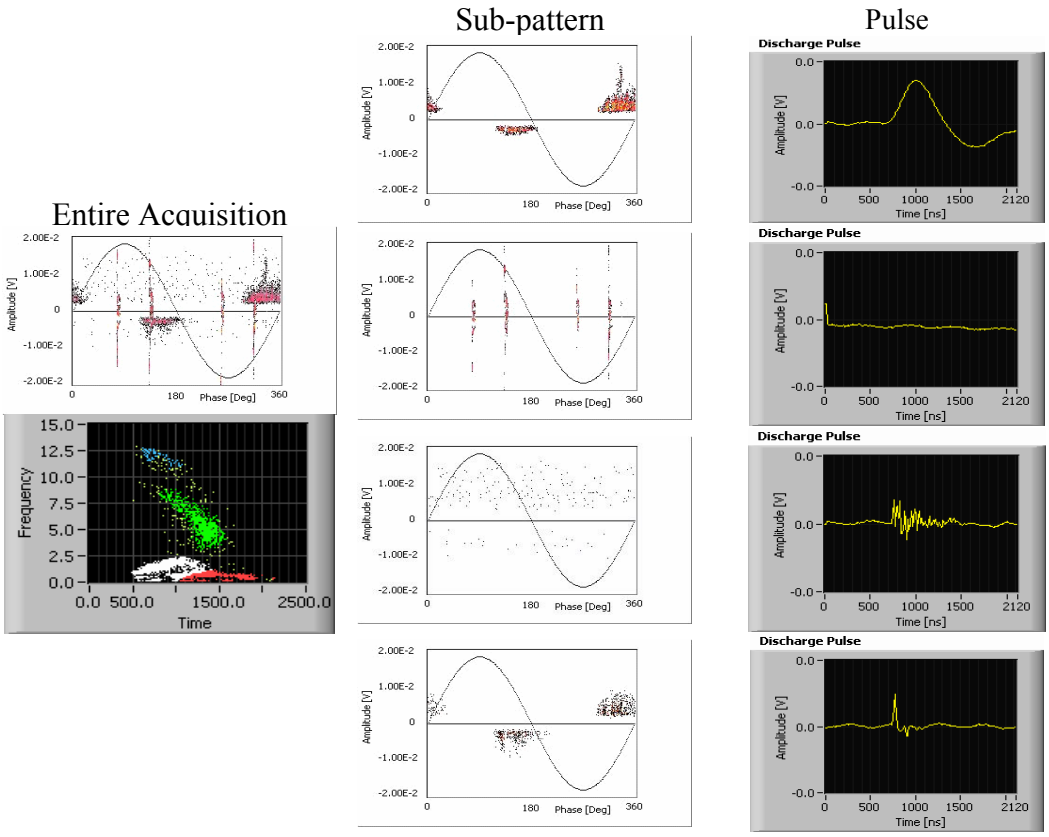

Fig. 33: Separation of clusters due to different PD sources [180]

7 CALIBRATION OF PD MEASURING CIRCUITS

Calibration Procedure

As discussed already in section 6 the transient voltage step appearing across the test object terminals as a result of a PD event is a measure of the apparent charge q_a. That means, each PD event causes a reading R_i proportional to q_a. To express R_i in terms of pC the scale factor S_f has to be determined by a specified calibration procedure. This is based on the injection of a well known calibrating charge q_0 in the test object terminals causing the reading R_0 of the PD instrument. Thus the scale factor can simply be expressed by:

$$S_0 = q_0 / R_0 \qquad (19)$$

Therefore, in case of a real PD tests the apparent charge q_a can be calculated from the reading R_i as:

$$q_a = S_f * R_i = q_0 * R_i / R_0 \qquad (20)$$

The calibration procedure recommended in IEC 60270 [9] is based on a simulation of the internal charge transfer from the PD site to the test object terminals by an external injection of artificial PD pulses [99, 101], as illustrated in Fig. 34.

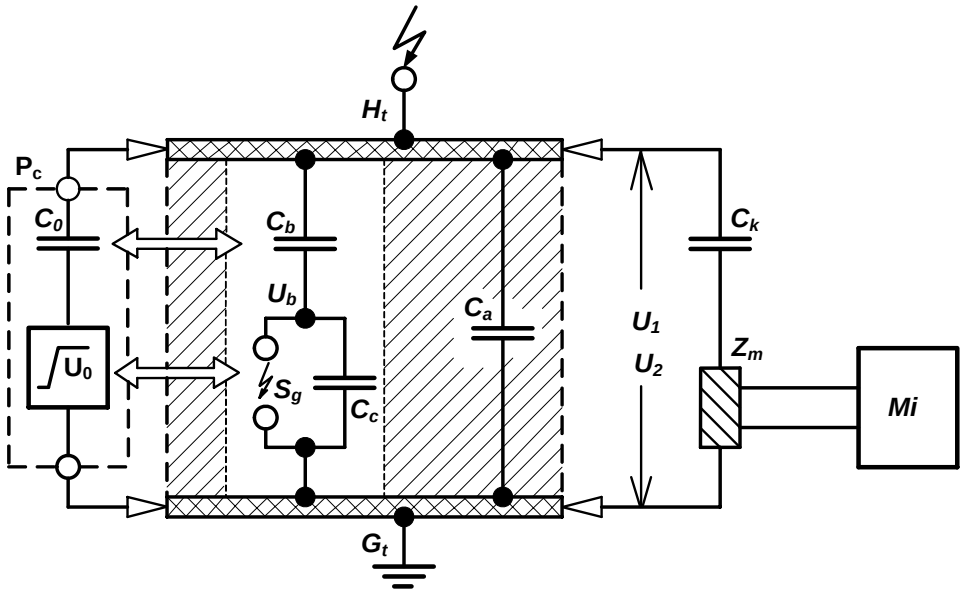

C_a – *virtual capacitance of the test object*
C_b – *stray capacitance of the PD source*
C_c – *internal capacitance of the PD source*
C_0 – *series capacitance of the calibrator*
S_g – *spark gap*
Pc – PD calibrator
C_k – *coupling capacitor*
Z_m – *measuring impedance*
U_0 – *voltage step created by the calibrator*
U_b – *voltage step created by the PD source*
U_1 – *voltage step across C_a due to the calibration*
U_2 – *voltage step across C_a due to a PD event*
H_t – *high voltage termination of the test object*
G_t – *grounded terminal of the test object*
M_i – *PD measuring instrument*

Fig. 34: Equivalent circuit for calibrating the apparent charge

Therefore, the PD calibrator is equipped with a pulse generator connected in series with a calibrating capacitor. To simulate the transient voltage across the PD defect the pulse generator creates equidistant voltage steps of known magnitudes U_0. If the value of the calibrating capacitor C_0 is much lower than the virtual test object capacitance C_a the injected calibrating charge can simply be expressed by:

$$q_0 = C_0 * U_0 = C_a * U_1 \qquad (21)$$

If now real PD events appear, the apparent charge is given by:

$$q_a = C_a * U_2 \qquad (22)$$

Introducing equation (21) in equation (22) the unknown value of C_a can be eliminated and we get:

$$q_a = q_0 * U_2 / U_1 \qquad (23)$$

Because the transient voltages U_2 and U_1 cause the corresponding readings R_i and R_0 equation (23) is equivalent to equation (20):

$$q_a = q_0 * R_i / R_0 \qquad (24)$$

Requirements for PD Calibrators

Usually hand-held and battery-powered calibrators are used. To design such devices it has to be taken into consideration that under realistic condition the breakdown voltage of PD defects may exceed few kV or even more. Furthermore, the stray capacitance C_b of the PD defect is usually less than one pF. Such calibrating parameters, however, cannot simply be realized at sufficiently high accuracy. Therefore, with respect to a cost-effective design of PD calibrators the following requirements are recommended:

1. Pulse shape parameters

From fundamental studies of PD phenomena it is known that the charge transfer from the PD site to the test object terminals is usually finished after few tens of nanoseconds. Therefore, the step pulse generator should have an equivalent rise time t_r, because the transfer of the calibrating charge via the calibrating capacitor C_0 is governed by t_r. Furthermore it has to be taken into account that the transferred pulse charge is proportional to the step pulse magnitude. Thus the magnitude and time to steady state of an occurring over- and undershoot as well as the steady state duration should also be specified. Based on practical experiences the impact of the step pulse shape on the uncertainty of the calibrating charge can be neglected if the following conditions are satisfied, see Fig. 35:

Rise time	: $t_r < 60$ ns
Time to steady state	: $t_s < 500$ ns
Steady state duration	: $t_d > 5$ µs
Overshoot	: $U_d < 0.1\ U_0$
Undershoot	: $U_t < 0.1\ U_0$

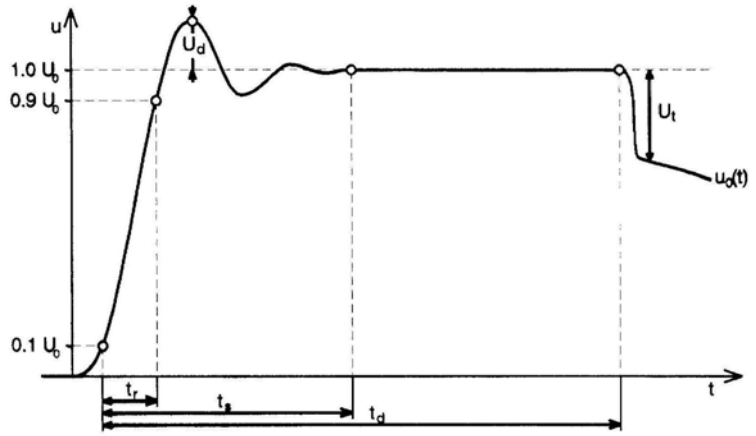

Fig. 35: Parameters recommended for the step pulse shape of PD calibrators [99]

2. Calibrating capacitor

The charge transferred from the PD calibrator via the calibrating capacitor C_0 to the virtual test object capacitor C_a as well as to the parallel connected coupling capacitor C_k can be expressed by:

$$q_c = \Delta U_0 * C_0 (1- C_0 /(C_0 + C_a + C_k)) \quad (25)$$

For the condition:

$$C_0 << C_a + C_k \quad (26)$$

the impact of $(C_a + C_k)$ on the pulse charge transferred from the output of the calibrator to the terminals of the test object can be neglected. Thus the well known values of C_0 and U_0 can be used to calculate accurately the calibrating charge:

$$q_c = q_0 = U_0 * C_0 \quad (27)$$

According to IEC 60270 [9] the following requirement should be satisfied:

$$C_0 < 0.1 (C_a + C_k) \quad (28)$$

The worst case arises for $C_a << C_k$ where the minimum test circuit capacitance is governed by the coupling capacitor C_k alone. Because this value should be chosen in the order of some 100 pF the maximum capacitance of C_0 should not exceed 100 pF in order to keep the calibrating error as low as possible. Common used battery-powered PD calibrators generate generally a maximum step voltage magnitude of $\Delta U_0 < 10$ *V*. Thus a maximum calibrating charge of $q_0 < 1000$ pC could be created under this condition. If higher magnitudes are desired it is recommended to increase the step pulse voltage magnitude accordingly but not the value of the calibrating capacitor. Otherwise the transferred pulse charge in compliance to equation (27) would be reduced and, additionally, deformation of the front region of the step pulse may appear, such as a creeping effect, so that the tolerances reported in Fig. 35 may not be satisfied.

Performance Tests of PD Calibrators

To verify the significant parameters of PD calibrators, such as the created pulse charge magnitude as well as the pulse shape parameters of the step pulse generator, IEC 60270 [9] demands a performance test. The procedure is based on the injection of the calibrating pulses into a measuring resistor R_m, see Fig.36a. Because the series connection of C_0 with R_m represents a high-pass filter, the voltage across R_m is differentiated, as obvious from Fig. 36b.

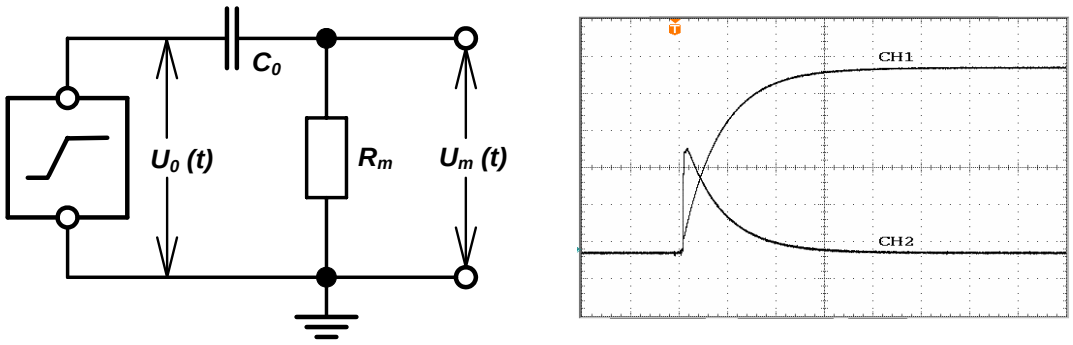

a) Measuring setup b) Characteristic voltages

CH1 – Input voltage u_0 (t) created by the pulse generator, scale: 100 mV/div
CH2 – output voltage u_m (t) across R_m, scale: 10 mV/div, time base: 20 ns/div
Measuring conditions: U_0 = 0.5 V, C_0 = 100 pF, q_0 = 50 pF, R_m = 50 Ω

Fig. 36: Calibration pulse fed into a measuring resistor

Therefore the time dependent voltage u_m *(t)* appearing across R_m has to be integrated in order to determine the magnitude of the calibrating charge:

$$q_0 = \int i_m(t) * dt = (1/R_m) * \int u_m(t) * dt \qquad (29)$$

For this an advanced digital technique is required having an adequate amplitude resolution of 10 bits or even higher and a sampling rate not less than of 500 MS/s, where the analogue band-width of the input amplifier should not be less than 50 MHz. Moreover it is reported in [102] that the band-width of the oscilloscope is not critical in the evaluation of the integral. However, since the procedure is numerical, a sufficient number of points must be available, which requires an oscilloscope with the capability of sampling in "equivalent time" or with sampling rate much higher than that which could be assumed to be sufficient on the basis of the Nyquist frequency. Finally, the transient characteristic of the input channel of the digital oscilloscope is very important with special reference to the settling time that shall be faster than the settling time of the charge signal. From a general point of view digital oscilloscopes calibrated according to the standard IEC 61083-1 are suitable for this test.

As an alternative for calibrating the PD calibrator the measuring resistor R_m shown in Fig. 36a can be substituted by a measuring capacitor C_m. Under this condition a voltage divider is formed by the series connection of C_0 and C_m. Thus the voltage drop across C_m represents a direct measure of the pulse charge to be calibrated.

For $C_0 << C_m$ equation (25) can be simplified as:

$$q_{cal} = U_0 * C_0 * (1- C_0 / C_m) = q_0 * (1- C_0 / C_m) \qquad (30)$$

For a charge transfer of more than 99 % of q_0 the following condition must be satisfied:

$$C_0 / C_m < 1 / 100; \qquad C_m > 100 * C_0 \qquad (31)$$

This means that a voltage divider ratio of 1: 100 is required, i.e. only 1 % of the voltage step U_0 appears across C_m. This value may become extremely low and is thus difficult to measure at sufficient uncertainty, in particular for calibrating charges below 10 pC. For better understanding let us consider the following quantitative example:

$C_0 = 100\ pF, \quad U_0 = 50$ mV, $\quad q_0 = C_0 * U_0 = 100$ pF $* 50$ mV $= 5$ pC

$C_m = 100 * C_0 = 10000\ pF, \quad q_m = q_0 = C_m * U_m$

From these assumptions follows the voltage step to be measured as low as $U_m = q_0 / C_m = 0.5$ mV, where a tolerance of only 0.015 mV can be accepted if an uncertainty of 3 % is desired. To increase the voltage step to be measured C_m should be reduced accordingly. This is possible if an "active integration circuit" is employed which ensures the transfer of the complete charge from the calibrator to the measuring capacitor C_m as reported in [99, 100], see Fig. 37.

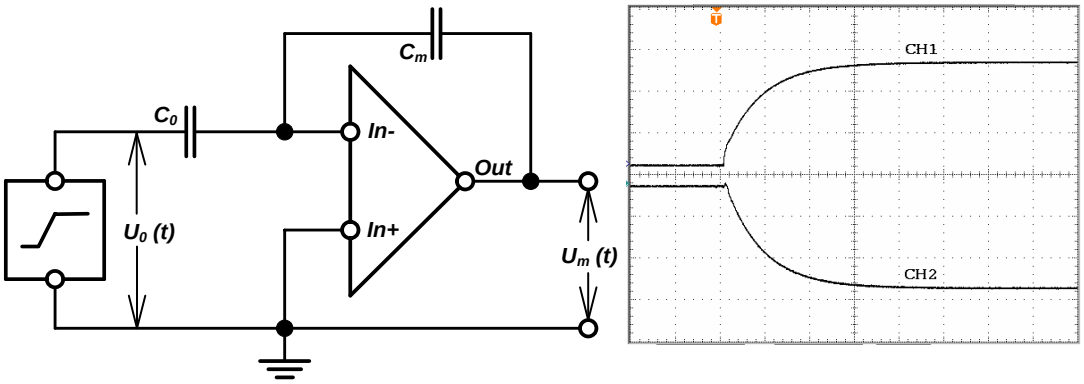

a) Measuring setup b) Characteristic voltages

CH1 – Input voltage u_0 (t) created by the pulse generator, scale: 100 mV/div
CH2 – output voltage u_m (t) of the differential amplifier, scale: 10 mV/div, time base: 20 ns/div
Measuring conditions: $U_0 = 0.5$ V, $C_0 = 100$ pF, $q_0 = 50$ pF, $C_m = 100$ pF

Fig. 37: Calibration pulse fed into an active integrator

At sufficient high common mode rejection of the differential amplifier the voltage magnitude appearing at the inverting input (In-) is always equal to that of the non-inverting input (In+), which is terminated to a fixed reference potential. Consequently, for $C_m = C_0$ the voltage step U_0 generated by the calibrator appears inverted at the output of the differential amplifier but at exact the same magnitude, i.e. $U_m = - U_0$. That

means the measurable pulse charge q_m which is stored in the measuring capacitor C_m is equal to the pulse charge q_0 to be determined:

$$q_m = \Delta U_m * C_m = q_0 = \Delta U_0 * C_0 \qquad (32)$$

If, for instance, $C_0 = C_m = 100\ pF$ is assumed a calibrating charge of $q_0 = 5\ pC$ would produce a voltage ramp of 50 mV, which can be measured precisely by the built-in peak detector of commercially available digital oscilloscopes, in particular if the averaging mode is applied. Due to practical experience an extended measuring uncertainty of

$$U_m < 0{,}03 q_0 + 0{,}5\ pC \qquad (33)$$

can be achieved by using the electronic integration principle presented here.

8 MAINTAINING THE PD DEVICE CHARACTERISTICS

General

The third edition of IEC 60270: 2000 [16] introduced the following three levels for maintaining the characteristics of PD measuring devices consisting of the coupling device, the PD instrument and the PD calibrator as well as the associated measuring connection leads:

1. The routine calibration of the complete PD measuring system connected to the HV test circuit that is performed prior to a PD test. This calibration provides the scale factor S_f of the system to be used in the test (or is used to adjust the reading of the instrument to obtain a direct reading of the PD magnitude, i.e. S_f should satisfy preferable values, such as 1, 2, 5, 10, 20….). For this routine calibration there are no major changes as compared to the IEC edition of 1981[8].

2. The determination of the specified characteristics of the complete PD measuring system which should be performed at least once a year or after major repair.

3. The calibration of the PD calibrator.

In general manufacturers of PD measuring devices provide the necessary guidelines for verification the specified technical parameters. Independent from such guidelines the third edition of IEC 60270 [9] recommends additional test procedures, where the results are recorded in a “Record of Performance (RoP)” established and maintained by the user. The RoP should include the following information:

1. Nominal characteristics (identification; operation conditions, measuring range, supply voltage)
2. Type test results
3. Routine test results
4. Performance test results (date and time)
5. Performance check results (date and time; result: passed/ failed: if failed: action taken)

Verifications of PD measuring systems and PD calibrators shall be performed once as acceptance tests. Performance tests shall be performed periodically or after any major repair, and at least every five years. Performance checks are performed periodically and at least once a year. In the following a brief survey on the tests recommended in IEC 60270 [9] for maintaining the characteristics of PD measuring systems and PD calibrators will be presented.

Maintaining the Characteristics of PD Measuring Systems

1. Type tests

These are to be done by the manufacturer and shall be performed for one PD measuring system of a series and shall at least include the determination of the following parameters:

1.1 The frequency dependent transfer impedance $Z(f)$ and the lower and upper frequencies f_1 and f_2 over a frequency range in which it has dropped to 20 dB from the peak pass-band value.

1.2 The scale factor k to calibrating pulses of at least three different pulse charge magnitudes ranging between 10 % and 100% of the full reading at a pulse repetition rate n around 100 s^{-1}. In order to prove the linearity of the PD measuring instrument the variation of k shall be less than 5 %.

1.3 The pulse resolution time T_r by applying calibration pulses of constant magnitude but decreasing time interval between consecutive pulses.

1.4 Pulse train response for pulse repetition rates N ranging between 1 s^{-1} and > 100 s^{-1} where the reading of the PD instrument should satisfy the tolerance band illustrated in Fig. 25.

2. Routine tests

These are to be done by the manufacturer and shall include all tests required in a performance test as listed below. Routine tests shall be performed for each measuring system of a series. If the test results are not available from the manufacturer, the required tests shall be arranged by the user.

3. Performance tests

These shall include the determination of the following parameters:

3.1 The frequency dependent transfer impedance $Z(f)$ and the lower and upper frequencies f_1 and f_2 over a frequency range in which it has dropped to 20 dB from the peak pass-band value.

3.2 The linearity of the scale factor k to be verified between 50 % of the lowest and 200 % of the highest specified PD magnitude. Using calibrating pulses of adjustable magnitude having a repetition rate of approximately $n = 100\ s^{-1}$, the scale factor k shall vary not more than 5 %.

4. Performance checks

These shall include the determination of the following parameters:

4.1 The transfer impedance $Z(f)$ at one frequency selected in the band-pass range in order to verify that the value deviates not more than 10 % from that one recorded in the performance test.

Maintaining the Characteristics of PD Calibrators

1. Type tests

These are to be done by the manufacturer and shall be performed for one PD calibrator of a series. Type tests shall include at least all tests required in a performance test. If results of type tests are not available from the manufacturer, the required tests for verification the technical parameters of PD calibrators shall be arranged by the user.

2. Routine tests

These are to be done by the manufacturer and shall include all tests required in a performance test. Routine tests are to be performed by the manufacturer for each measuring system of a series. If the test results are not available from the manufacturer, the required tests shall be arranged by the user.

3. Performance tests

These shall include the determination of the following parameters:

3.1 The actual magnitude of the pulse charge q_0 for all nominal settings, where a measuring uncertainty within 5 % or 1 pC, whichever is greater, is recommended.

3.2 Rise time t_r of the voltage step U_0, where a measuring uncertainty within 10 % is recommended.

3.3 Pulse repetition frequency N, where a measuring uncertainty within 1 % is recommended.

4. Performance checks

These include the determination of the actual magnitude of the calibrating charge q_0 for all nominal settings, where a measuring uncertainty within 5 % or 1 pC, whichever is greater, is recommended.

9 SUMMARY

Partial discharges (PD) have been recognized as harmful for electrical insulation at the beginning of the last century when the HV technology was introduced for the generation and transmission of electrical power. Since that time numerous papers and books appeared dealing with physical and technical aspects of PD recognition. First industrial PD tests of HV apparatus were performed at the beginning of 1940 based on the radio influence voltage (RIV) measurement according to NEMA 107.

In the 1960`s the IEC Technical Committee No. 42 decided the introduction of the PD quantity apparent charge for quality assurance tests of HV apparatus. This quantity was first defined in the IEC publication 270 issued in 1968. The second edition of IEC 270, which appeared in 1981, recommended the measurement of the "largest repeatedly occurring apparent charge". This PD quantity is based on a specified PD pulse train response of the PD instrument.

The third edition of IEC 60270, published in December 2000, covers besides the requirements for the classical analogue technique also specific requirements for digital measuring instruments. Moreover, recommendations for maintaining specific characteristics of PD measuring systems and calibrators are presented. In this context it seems noticeable that currently the standard IEC 62478 is under preparation, which covers the electromagnetic (UHF) and acoustical PD detection. These non-conventional methods, however, are outside of the scope of this brochure.

For better understanding the background of IEC 60270 the CIGRE Working Group D1.33 "High-Voltage Testing and Measuring Techniques" decided the edition of a Technical Brochure intended as a guideline for electrical engineers dealing with conventional electrical PD measurements for quality assurance tests of HV apparatus. The issues of this brochure can be summarized as follows:

1. Conventional electrical PD measurements have been proven as an indispensable tool to trace dielectric imperfections in HV apparatus which may lead to an inevitable breakdown. Therefore, the increased quality requirements for modern insulation systems as well as the enhancement of the electrical field strength and last but not least the desired enlargement of the lifetime of HV apparatus requires an early detection of severe PD defects due to design failures and/or poor assembling work.

2. For better understanding the design criteria of PD measuring circuits a sufficient knowledge of the very complex PD nature is required. Therefore this brochure summarized first some fundamentals of the PD occurrence where the various topics are treated in a highly simplified manner.

3. The shape of original PD current pulses is strongly distorted if traveling from the PD site to the terminals of the test object. Contrarily to this appears the current-time integral of PD pulses detectable across the test object terminals more or less invariant. Therefore the charge of PD pulses is considered as the most suitable parameter for reproducible and comparable PD measurements.

4. The charge temporarily stored in the virtual test object capacitance is called “apparent charge”, because it is only a small fraction of the true charge created inside the PD source. Consequently, critical values of the apparent charge specified in the relevant apparatus standards are not based on the physics of discharges but on long-term experiences of experts.

5. Besides the measurement of the apparent charge IEC 60270 recommends the evaluation of additional PD quantities, such as the PD inception and extinction voltage, as well as the pulse repetition rate, the pulse repetition frequency, the phase angle, the average discharge current, the discharge power and the quadratic rate.

6. The apparent charge measurement is based on the quasi-integration of the PD pulses captured from the terminals of the test object. For this the measuring frequency is tuned in a range where the density of the amplitude-frequency spectrum of the PD pulses is nearly constant. For the evaluation the “largest repeatedly occurring apparent charge” the pulse train response of the PD instrument is specified accordingly.

7. Due to the fast progress in digital signal processing this technique is nowadays widely used. The main feature of a computerized PD instrument is the ability to store the apparent charge pulses, the instant time of occurrence, the instantaneous test voltage magnitude and the phase angle of each PD event. This ensures a visualization of the phase-resolved PD pattern in a replay-mode, i.e. similar to the video recorder technology. Moreover, statistical tools can be applied for an in-depth analysis and thus an identification and classification of the very complex PD events. Additionally, PD sites can be localized, for instance in GIS or long power cables using the time domain reflectometry. The digital technique is also capable for an effective de-noising of PD signals.

8. The calibration of PD measuring circuits specified in IEC 60270 is based on a simulation of the internal charge transfer from the PD site to the test object terminals by an external injection of artificial PD pulses. These are created usually by a hand-held battery-powered calibrators equipped with a step pulse generator in series with a calibrating capacitor.

9. To verify the pulse charge and time parameters of calibrating pulses IEC 60270 demands a performance test. This is based on the injection of the calibrating pulses into a well known resistor and measurement of both, the determination of the voltage-time integral and the duration of the resulting voltage pulse. As an option the calibrating charge can also be determined by an injection of the charge in a well known measuring capacitor and measuring the voltage ramp across this capacitor. To ensure the full charge transfer from the calibrator to the measuring capacitor the application of an electronic integration is recommended.

10. Maintaining the characteristics of PD measuring facilities IEC 60270 recommends the following procedures:

- Routine calibration of the complete PD measuring system connected to the HV test circuit to provide the scale factor required for the calculation of the apparent charge from the reading of the PD instrument. This should be performed prior to each PD test.

- Determination of the specified characteristics of the complete PD measuring system. This should be performed at least once a year or after a major repair.

- Calibration of the PD calibrator. This should be performed at least once a year or after a major repair.

11. Manufacturers of PD measuring devices provide in general the necessary guidelines for the verification of the specified technical parameters. Independent from such guidelines additional test procedures are recommend in IEC 60270, where the results shall be maintained by the user in a "Record of Performance (RoP)". This document shall include the nominal characteristics (identification; operation conditions, measuring range, supply voltage), the results of type tests, routine tests and performance tests as well as the results of performance checks, including date, time, passed/ failed, action taken.

12. Verifications of PD measuring systems and PD calibrators shall be performed once as acceptance tests. Performance tests shall be performed periodically or after any major repair, and at least every five years. Performance checks shall be performed periodically and at least once a year.

10 REFERENCES

[1] NEMA 107: Methods of Measuring Radio Noise, first edition (1940)

[2] NEMA 107 (R 1971): Methods of Measurement for Radio Influence Voltage (RIV) of High-Voltage Apparatus, second edition (1964)

[3] IEC-Publication 1: Specification for CISPR radio interference measuring apparatus for the frequency range 0.15 Mc/s to 30 Mc/s (1961)

[4] CISPR 16-1: Specification for radio disturbance and immunity measuring apparatus and methods – Part 1: Radio disturbance and immunity measuring apparatus (1993)

[5] Harrold, R.T.: Dakin, T.W.: The Relationship Between the Picocoulomb and the Microvolt for Corona Measurements on HV Transformers and other Apparatus. IEEE Transactions on Power Apparatus and Systems, PAS-92 (1973) 1 pp. 187-198

[6] Vaillancourt, G.H., Dechamplain, A., Malewski, R.: Simultaneous Measurement of Partial Discharge and Radio Interference Voltage. IEEE Electrical and Electronic Measurement and Test Instrument Conference, Ottawa (1981)

[7] IEC-Publication 270: Partial discharge measurement, first edition (1968)

[8] IEC Publication 270: Partial discharge measurement, second edition (1981)

[9] IEC 60270: High-voltage test techniques – Partial discharge measurements, third edition (2000)

[10] IEC 62478: High-voltage test techniques – Measurement of partial discharge by electromagnetic and acoustic methods (first edition, 200-xx)

[11] Lichtenberg, G. Ch.: De nova methodo naturam ac motum fluidi electrici investigandi. Novi Commentarii Societatis Regiae Scientiarum Gottingensis, Vol. 8 (1777), p. 168 (part 1) and Commentationes Societatis Regiae Scientarum Gottingensis 1 (1778) p. 65 (part 2)

[12] Reitlinger E.: Zur Erklärung der Lichtenbergschen Figuren. Sitzungsberichte der Akademie der Wissenschaften, Mathematisch-naturwissenschaftliche Klasse 41 (1860) p. 385

[13] Rood, O.N.: On the Study of the Electric Spark by the Aid of Photography. American Journal of Science & Arts II-33 (1862) p. 219

[14] Blake, W.: On a Method of Producing by the Electric Spark Figures similar to those of Lichtenberg. American Journal of Science & Arts, II-49 (1870) p. 289

[15] Wiedemann, G.: Die Lehre von der Elektrizität. Vol. 4-1, Vieweg, Braunschweig (1885) p. 761

[16] Toepler, M.: Über gleitende Entladung längs reinen Glasoberflächen. Annalen der Physik und Chemie 66 (1898) pp. 1061

[17] Holtz, W.: Über die Lichtenbergschen Figuren und ihre Entstehung. Zeitschrift für Physik 6 (1905) p. 319

[18] Toepler, M.: Zur Kenntnis der Gesetze der Gleitfunkenbildung. Annalen der Physik 21 (1906) pp. 193-222

[19] Toriyama, Y: Dust Figures in Liquid Insulators. Physical Review 37 (1931) p. 619

[20] Merrill, F.H., Hippel, A.: The Atomphysical Interpretation of Lichtenberg Figures and Their Application to the Study of Gas Discharge Phenomena. Journal of Applied Physics, 10 (1939) pp. 873-887

[21] Lemke, E.: Durchschlagmechanismus und Schlagweite-Durchschlagspannungs-Kennlinien von inhomogenen Luftfunkenstrecken bei Schaltspannungen. Ph. D. Thesis, TU Dresden (1967)

[22] Hauschild, W.: Zum Öldurchschlag in inhomogenen Feld bei Schaltspannungen. Ph. D. Thesis TU Dresden (1970)

[23] Takahashi, Y.: Two hundred Years of Lichtenberg Figures. Journal of Electrostatics 6 (1979) pp. 1-13

[24] Petersen, W.: Hochspannungstechnik. Ferdinand Enke Verlag, Stuttgart (1911)

[25] Wagner. K.W.: The Physical Nature of Electrical Breakdown in Solid Dielectrics. Journal of American Institution of Electrical Engineering 61 (1922) pp. 1034

[26] Schumann, W.O.: Elektrische Durchbruchfeldstärke von Gasen. Springer-Verlag, Berlin (1923)

[27] Schwaiger, A.: Elektrische Festigkeitslehre. Springer-Verlag, Berlin (1925)

[28] Geiger, H. Scheel, K.: Handbuch der Physik, Vol. 14 – Elektrizitätsbewegung in Gasen. Springer-Verlag, Berlin (1927)

[29] Burstyn: Die Verluste der geschichteten Isolierstoffe. ETZ 49 (1928) pp. 1285-1291

[30] Mason, J.H.: The Deterioration and Breakdown of Dielectrics Resulting from Internal Discharges. Proceedings IEE 98 (1951) pp. 44-59

[31] Schering, H.: Brücke für Verlustmessungen. Tätigkeitsbericht der Physikalisch-Technischen Reichsanstalt (1919)

[32] Peters, J.F.: The Klydonograph. Electrical World, 83 (1924) p. 769

[33] Müller, H.: Neuere Messungen mit dem Klydonographen. Hescho-Mitteilungen (1927) 34, p. 1049

[34] Lloyd, W.L., Starr, E.C.: Untersuchung der Wechselstromkorona mit dem Kathodenstrahl-Oszillographen. ETZ 49 (1928) pp. 1276

[35] Arman, A.N., Starr, A.T.: The Measurement of Discharges in Dielectrics. Journal IEE 79 (1936) pp. 67-81 and pp. 88-94

[36] Koske, B.: Prüfung der Isolation von Hochspannungs-Freileitungen. Elektrizitätzwirtschaft 36 (1938) 11, p. 291

[37] McMillan, F.O., Starr, E.C.: The Influence of the Polarity of High-Voltage Discharges. Journal AIEE 49 (1930) pp. 859

[38] Gemant, A., Philippoff, W.: Die Funkenstrecke mit Vorkondensator. Zeitschrift für Technische Physik, 13 (1932) 9, pp. 425-430

[39] Loeb, L.B.: The Energy of Formation of Negative Ions in O_2. Physical Review 48 (1935) p. 684

[40] Trichel, G.W.: Mechanism of Negative Point to Plane Corona near Onset. Physical Review 54 (1938), pp. 1078-1084

[41] Loeb, L.B. Basic Processes of Gaseous Electronics. Wiley, London (1939)

[42] Marx, E.: Hochspannungs-Praktikum. Springer-Verlag, Berlin (1952)

[43] Meek, J.M., Craggs, J.D.: Electrical Breakdown of Gases. Wiley & Sons, London (1953)

[44] Gänger, B.: Der elektrische Durchschlag von Gasen. Springer-Verlag, Berlin (1953)

[45] Roth, A. Hochspannungstechnik. Springer-Verlag, Wien (1959)

[46] Lesch, G.: Lehrbuch der Hochspannungstechnik. Springer-Verlag, Berlin (1959)

[47] Heintz, W.: Untersuchung des hochfrequenten Spektrums periodischer Entladungen. Zeitschrift für angewandte Physik 11 (1959) 2, pp. 51-57

[48] Veverka, A., Hon, A.: Erweiterte Ersatzschaltung für innere Teilentladungen im Dielektrikum. Elektr. Obzor. 53 (1964) 1 pp. 14-18

[59] Raether, H.: Electron Avalanches and Breakdown in Gases. Butterworths, London (1964)

[50] Kreuger, F.H.: Discharge Detection in High-Voltage Equipment. Temple Press, London (1964)

[51] Heller, B. Chladek, J.: Das kapazitive Ersatzschema für Koronavorgänge im festen Dielektrikum. Acta Technica CSAV 10 (1965) 6, pp. 613-622

[52] Bartnikas, R., DÓmbrain, G.L.: A Study of Corona Discharge Rate and Energy Loss in Spark Gaps. IEEE Transactions Power Systems and Apparatus, PAS-84 (1965) 9, pp. 770-779

[53] Bailey, C.A.: A Study of Internal Discharges in Cable Insulation. IEEE Transactions on Electrical Insulation, EI-31 (1966) 9, pp 360-366

[54] Schwab, A., Zentner, R.: Der Übergang von der impulsförmigen in die impulslose Koronaentladung. ETZ-A 89 (1968) 17, pp. 402-407

[55] Recognition of Discharges. Proceedings of CIGRE, Electra 11 (1969) p.61

[56] Schwab, J.A. Hochspannungsmesstechnik. Springer-Verlag, Berlin (1969)

[57] Galand, J. Golinski, J., Labus-Nawrat, K.: La détection des décharges partielles. Rev. Gén. Electr. 81 (1972) 12, pp. 844-853

[58] Csernátony-Hoffer, A.: Zerstörungsfreie Prüfung von Hochspannungsisolierungen. ETZ-A 93 (1972) 6, pp. 326-335

[59] Pilling, J.: Ein Beitrag zur Interpretation der Lebensdauerkennlinien von Feststoffisolierungen. Habilitation Thesis TU Dresden (1976)

[60] Mason, J.H.: Discharges. IEEE Transactions on Electrical Insulation, EI-13 (1978) 4, pp. 211-238

[61] Fujimoto, N., Boggs, S.A., Madge, R.C.: Electrical transients in gas-insulated switchgear. Transactions of the March 1981 Meeting of the Canadian Electric Association.

[62] Boggs, S.A., Stone, G.C.: Fundamental Limitations in the Measurement of Corona and Partial Discharge. IEEE Transactions on Electrical Insulation EI-17 (1982) 2, pp143-150

[63] Tanaka, T.: Internal Partial Discharge and Material Degradation. IEEE Transactions on Electrical Insulation, EI-26 (1986) 6, pp. 899-905.

[64] Beyer, B., Boeck, W., Möller, K., Zaengl, W.: Hochspannungstechnik. Theoretische und praktische Grundlagen für die Anwendung. Springer-Verlag, Berlin (1986)

[65] Kreuger, F. H. Partial Discharge Detection in High-Voltage Equipment. Heywood, London (1969) and Butterworths, London (1989).

[66] Morshuis, P.H.F.: Partial Discharge Mechanisms. Ph.D. Thesis TU Delft (1993)

[67] Ramachandra, B.: Characterization of Partial Discharge Pulses in Artificial Voids in Thin Polypropylene Films. Ph. D Thesis., I.I.Sc. Bangalore (1997)

[68] Quinn, G.E.: A Method for Detecting the Ionization Point on Electrical Apparatus. AIEE Transactions on Electrical Engineering, 59 (1940) pp 680-682

[69] Mole, G.: Design and Performance of a Portable AC Discharge Detector. Electrical Research Association (ERA), Report V/T 115 (1952)

[70] Mole, G.: The ERA Portable Discharge Detector. CIGRE-Session Paris (1954) paper No. 105, appendix I

[71] Dakin, T.W., Malinaric, P.J.: A Capacitive Bridge Method for Measuring Integrated Corona Charge Transfer and Power Loss per Cycle. AIEE Transactions on Power Apparatus and Systems, PAS-79 (1960) pp. 648-653

[72] Kind, D.: Grundlagen der Messeinrichtung für Korona-Isolationsprüfungen ETZ-A 84 (1963) 24, 24, pp. 781-794.

[73] Widmann, W.: Beitrag zur Bestimmung der Messempfindlichkeit bei Teilentladungsprüfungen von Hochspannungsgeräten. AEG-Mitteilungen 55 (1966) 1, pp. 28-39

[74] Dakin, T. W., Works, C. N., and Miller, R. L.: Utilization of Peak-Reading Voltmeters and Recorders for Corona Measurement. IEEE Transactions on Electrical Insulation, EI-2 (1967) 2, pp. 75–82

[75] IEEE Committee Report: Guide for Calibration of Test Equipment and Circuits for Measurement of Corona Pulses. IEEE Transactions on Power Apparatus and Systems, PAS-86 (1967) 10, pp. 1185–1191

[76] Neudert, E. Porzel, R.: Ein oszillografisches Verfahren zum Beurteilen von Teilentladungen. ELEKTRIE 22 (1968) 9, 360-362

[77] Lemke, E.: Ein neues Verfahren zur breitbandigen Messung von Teilentladungen. ELEKTRIE 23 (1969) 11, pp 468-469

[78] Mole, G.: Basic Characteristics of Corona Detector Calibrators. IEEE Transactions on Power Apparatus and Systems, PAS-89 (1970) pp. 198-204

[79] Praehauser, T.: Teilentladungsmessungen an Hochspannungsapparaten mit der Brückenschaltung. Bulletin SEV 64 (1973) pp. 1183-1189

[80] Praehauser, T.: The calibration of PD Measuring Circuits. 2nd ISH Zürich (1975) paper 32-07

[81] Dembinski, E. M., Douglas, J. L.: Calibration and Comparison of Partial Discharge and Radio-Interference Measuring Circuits. IEE Proceedings, Vol. 115 (1968) 9, pp. 1332–1340

[82] Schwab, A., Zentner, R.: Der Übergang von der impulsförmigen in die impulslose Koronaentladung. ETZ-A 89 (1968) 17, pp 402-407

[83] CIGRE WG 21-03: Significance of Discharge Detection. Electra 11 (1969) pp. 53–60

[84] CIGRE WG 21-03: Recognition of Discharges. Electra 11 (1969) pp. 61–98

[85] Bartnikas, R.: Effect of Pulse Rise Time on the Response of Corona Detectors. IEEE Transactions on Electrical Insulation, EI-7 (1972) 1, pp. 3–8

[86] Lemke, E: Beitrag zur elektrischen Messung von Teilentladungen unter besonderer Berücksichtigung eines Verfahrens zur breitbandigen Erfassung der Summenladung. Habilitation Thesis TU Dresden (1975)

[87] Bartnikas, R. ,McMahon, E. J.: Corona Measurement and Interpretation. Eng. Dielectrics, Vol. 1, American Society for Testing and Materials, STP 669 (1979)

[88] Carter, W. J.: Practical Aspects of Apparent Charge Partial Discharge Measurements. IEEE Transactions on Power Apparatus and Systems, PAS-101 (1982) 7, pp. 1985–1989

[89]Lemke, E.: A New Approach to Characterize the Response of PD Measuring Circuits. 4th ISH Athens (1983) paper 63.11

[90]Brand, U., Muhr, M.: New Investigations on the Measurement of Partial Discharge (PD) and Radio Interference Voltage (RIV) in High-Voltage Engineering. 4th ISH Athens (1983) paper 63.13

[91] Huang, S. J., Lowder, S. M., Sarkinen, S. H., Chartier, V. L.: Evaluation of Partial Discharge Measurement Circuits and Associated Calibration Techniques. IEEE Transactions on Power Apparatus and Systems, PAS-104 (1985) 2, pp. 407–415

[92] Vallancourt, G., Malewski, R., Train, D.: Comparison of three Techniques of Partial Discharge Measurement in Power Transformers. IEEE Transactions on Power Apparatus and Systems, PAS-104 (1985) 4, pp. 900-909

[93] Schon, K: Konzept der Teilentladungsmessung bei Teilentladungsprüfungen. ETZ Archiv 8 (1986) 9, pp. 319-324

[94] Zaengl, W.S., Osvath, P.: Correlation between the Bandwidth of PD Detectors and its Inherent Integration Errors. ISEI Washington DC (1986)

[95] Kurrat, M., Peier, D.: Wideband Measurement of Partial Discharges for Fundamental Diagnosis. 7th ISH Dresden (1991) paper 71.02

[96] Niemeier, L., Fruth, B., GutfleischF.: Simulation of Partial Discharges in Insulation Systems. 7th ISH Dresden (1991) paper 71.05

[97] Moshuis, P.H.F.: Partial Discharge Mechanisms. Ph.D. Thesis TU Delft (1993)

[98] König, D., Narayana, R.: Partial Discharges in Electrical Power Apparatus. VDE-Verlag (1993)

[99] Lemke, E. Schmiegel, P., Elze, H., Russwurm, D.: Experience in the Calibration Technique for PD Calibrators. 3rd European Conference on High Voltage Measurements and Calibration, Milan (1996)

[100] Lukas, W., Schon, K., Lemke, E., Elze, H.: Comparison of Two Techniques for Calibrating PD Calibrators. 10th ISH Montreal (1997)

[101] Lemke, E.: Moderne TE-Meßsysteme und ihre Kalibrierung. HIGHVOLT Kolloquium, Dresden (1997) paper 3.7, pp. 95-106

[102] Cherbaucich, C. Rizzi, G., Gobbo, R., Pesavento, G., Saracco, O., Sardi, A.: Partial Discharge Calibrators: Practical Experience in their Calibration. ERA Conference on High Voltage Measurements and Calibration, London (1998)

[103] Borsi, H.: Verfahren zur Messung von Teilentladungen an Hochspannungskabeln unter Berücksichtigung des Einflusses der Kabeldaten, Ankopplungsvierpole und Messsysteme. Ph.D. Thesis, TU Hannover (1976)

[104] Lemke, E.: A new Method for PD Measurement of Polyethylene Insulated Power Cables. 3rd ISH Milan (1979) paper 43.13

[105] Borsi, H.: Möglichkeiten und Grenzen der Ortung von Teilentladungen an kunststoffisolierten Hochspannungskabeln. Habilitation Thesis, TU Hannover (1979)

[106] Stone, G.C., Boggs, S.A.: Propagation of partial discharge pulses in shielded power cables. Conference on Electrical Insulation and Dielectric Phenomena, IEEE Publication 82CH1773-1 (1982) paper V-6, pp. 275-280

[107]Beyer, M., Kamm, W., Borsi, H. Feser, K.: A New Method for Detection and Location of Distributed PD in High Voltage Cables. IEEE Transactions on Power Apparatus and Systems, PAS-101 (1982) pp. 3431-3437

[108] Osvath, P., Biasutti, G., Zaengl, W.S.: Zur Ortung und Beurteilung von Teilentladungen an Kunststoff-Hochspannungskabeln. Bulletin ASE/UCS78 (1987) pp. 482-487

[109] IEC60885-3: Electrical test methods for electric cables – Part3: Test methods for partial discharge measurements on lengths of extruded power cables (first edition 1988, second edition 2003)

[110] Hartill, E. R., Smith, L., James, R. E., Taylor, F. W., Ryder, D. H.: Some Aspects of Internal Corona Discharges in Transformers. CIGRE Session Paris (1962) paper 102

[111] Brown, R. D.: Corona Measurement on High-Voltage Apparatus Using the Bushing Capacitance Tap. IEEE Transactions on Power Apparatus and Systems, Vol. PAS-84 (1965) pp. 667–671

[112] Gänger, B. and Vorwerk, H. J. "Ionization Measurements on Transformers," The Brown Boveri Review, vol. 54, no. 7, pp. 355–367, July 1967.

[113] Fryxell, J., Agerman, E., Grundmark, B., Hessen, P., Lampe, W.: Performance of Partial Discharge Tests on Power Transformers. CIGRE Session Paris (1968) paper 12-04

[114] Wetzel, R. E., Praehauser, T. C.: Measurement of Partial Discharge on Transformers and Their Elements paper. CIGRE Session Paris (1968) paper 12-10

[115] Gailhofer, G., Kury, H., Rabus, W.: Partial Discharge Measurements on Power Transformer Insulation, Principles and Practice. CIGRE Session Paris (1968) paper 12-15

[116] James, R. E.: Discharge Detection in High-Voltage Power Transformers. Proceedings IEE, Vol. 117 (1970) 7, pp. 1352–1362

[117] CIGRE WG 12.01: Measurement of Partial Discharges in Transformers. ELECTRA19 (1971) pp. 13–65

[118] Dix, J. W., Hickling, G. H., and Raju, B. P. "Partial Discharge Measurement and its impact on Alternating Over-Potential Tests on Transformers," IEE Conference on Diagnostic Testing of HV Power Apparatus in Service, London, England, Conference Digest, Mar. 6–8 (1973) pp. 31-39.

[119] Douglas, J. L.: Calibration of Circuits for Measuring Partial Discharges in EHV Transformers. IEE Conference on Diagnostic Testing of HV Power Apparatus in Service. London (1973) pp. 40–47

[120] Douglas, J. L., Pratt, F. C., Rushton, F.: A Critical Assessment of Methods of Measuring Partial Discharges in EHV Transformers. CIGRE Session Paris (1974) paper 12-03

[121] CIGRE WG 12.01: Measurement of Partial Discharges in Transformers. ELECTRA 47 (1976) pp. 37–47

[122] Corvo, A. M.: Diagnostic Technique and Proceedings of Preventive Maintenance of Large Transformers. CIGRE Session Paris (1982) paper 12-11

[123] Baehr, R., Breuer W., Flottmeyer, F., Kotschnigg, J., Müller, R., Nieschwietz, H.: Diagnostic Techniques and Preventive Maintenance Procedures for Large Transformers," CIGRE Session Paris (1982) paper 12-13

[124] James, R. E., Trick, F. E., Phung, B. T., White, P. A.: Interpretation of Partial Discharge Quantities as Measured at the Terminals of HV Power Transformers. IEEE Transactions on Electrical Insulation, El-21 (1986) No. 4, pp. 629–638

[125] Fuhr, J., Haessig, M., Boss, P, Tschudi, D., King, R.A.: Detection and Localization of Internal Defects in the Insulation of Power Transformers. IEEE Transaction on Electrical Insulation, EI-28 (1993) 6

[126] CIGRE JWG 15/21/33-20: Progress on High-Voltage Monitoring Systems for In-service Power Apparatus. CIGRE Session Paris (1996)

[127] Wenzel, D., Borsi, H., Gockenbach, E.: A new Approach for Partial Discharge Recognition on Transformers On-site by means of Genetic Algorithms. IEEE International Symposium on Electrical Insulation (1996) pp. 57-60

[128] Fuhr, J.: Non-Standard PD-Measurements-Tool for Successful PD-Source Identification in the Laboratory. 13th ISH Delft (2003) paper P.02.07

[129] Werle, P., Akbari, A., Gockenbach, E., Borsi, H.: An Enhanced System for Partial Discharge Diagnosis on Power Transformers. 13th ISH Delft (2003) paper P.11.09

[130] Russwurm, D., Boltze, M.: Combined RIV and PD Measurement to Satisfy the Various Needs of Transformer Testing. 13th ISH Delft (2003)

[131] Matikainen, K: Some Observations upon Distributions of Partial Discharge Pulses measured with a Multi-Channel Analyser. CIGRE Session Paris (1968) paper 21-06

[132] Bartnikas, R.: A Simple Pulse-high Analyzer for Partial Discharge Measurements. IEEE Transactions Instrumentation and Measurement, IM-18, (1969) pp. 341-345

[133] Bartnikas, R.: Use of a Multi-channel Analyzer for Corona Pulse-Height Distribution Measurements on Cables and other Electrical Apparatus. IEEE Transactions on Instrumentation and Measurement, IM-22 (1973) 4, pp. 403–407

[134] Austin, J., James, R.E.: On-line Digital Computer System for Measurements of Partial Discharges in Insulation Structures. IEEE Transactions on Electrical Insulation, EI-11 (1976)

[135] Tanaka, T., Okamoto, T.: A Minicomputer-based Partial Discharge Measurement System. IEEE International Symposium on Electrical Insulation, Philadelphia (1978) pp. 86-89

[136] Kranz, H.G.: Partial Discharge Evaluation of Polyethylene Cable-material by Phase Angle and Pulse Shape Analysis. IEEE Transaction on Electrical Insulation, EI-17 (1982) pp. 151-155

[137] Muhr, M., Scheucher, W.: Computer-Aided Measurement of Partial Discharges. 4th ISH Athens (1983) paper 63.12

[138] Haller, R. Gulski, E.: Automatisierte Erfassung und Verarbeitung von TE-Signalen. Elektrie 38 (1984) 10, pp. 383-385

[139] Rochon, F., Malewski, R. Vallancourt, G.: Acquisition and Processing of PD Measurement During Power Transformer Testing. Conference on Dielectric Phenomena, Claymont (1984) pp. 546-554

[140] Okamoto, T., Tanaka, T.: Novel PD-Measurement Computer Aided Measurement System. IEEE Transactions on Electrical Insulation EI-21 (1986) pp. 1015-1019

[141] Wooton, R.E.: Computer Assistance fort he Performance and Interpretation of High Voltage AC Discharge Tests. 5th ISH Braunschweig (1987) paper 41.12

[142] Kreuger, F.H., Gulski, E.: Automatisiertes Messsystem zur Erfassung von Teilentladungs-Kenngrößen für die Beurteilung elektrischer Isolierungen. Technisches Messen, 56 (1989) 3, pp. 124-129

[143] Van Brunt, R.J.: Stochastic Properties of Partial-Discharge Phenomena. IEEE Transactions on Electrical Insulation, 26 (1991) 5

[144] Gulski, E.: Computer-Aided Recognition of Partial Discharges Using Statistical Tools. Ph.D. Thesis TU Delft (1991)

[145] Kranz, H.G., Krump, R.: Partial Discharge Diagnosis Using Statistical Optimization on a PC-based System. IEEE Transaction on Electrical Insulation, EI-27 (1992) pp. 93-98

[146] Ward, H.W.: Digital Techniques for Partial Discharge Measurements. IEEE Transaction on Power Delivery, 7 (1992) pp 469-479

[147] Alsheikly, A. Guzman, H., Kranz, H.G.: A New Tool Through Computer Simulation Calculation Using Expanded Partial Discharge Equivalent Circuit. 4th International Conference on Conduction and Breakdown in Solid Dielectrics, Sestri Levante, Italy (1992) pp. 176-180.

[148] Kreuger, F.H., Gulski, E., Krivda, A.: Classification of Partial Discharges. IEEE Transactions on Electrical Insulation, EI-28 (1993) 6, pp. 917-928

[149] Satish, L., Zaengl, W.: Artificial Neural Networks for Recognition of 3-D Partial Discharge Patterns. IEEE Transactions on Dielectrics and Electrical Insulation, 1 (1994) 2, pp. 265-275

[150] Fruth, B., Gross, D.W.: Combination of Frequency Spectrum Analysis and Partial Discharge Pattern Recording. IEEE International Symposium on Electrical Insulation, Pittsburgh (1994) pp. 296-300

[151] Hoof, M., Patsch, R.: Analyzing Partial Discharge Pulse Sequences – A New Approach to Investigate Degradation Phenomena. IEEE International Symposium on Electrical Insul89ation, Pittsburg (1994) pp. 327-331

[152] Poittevin, J., Andre, P.: New Digital Discharge Measurements on Transformers. CIGRE Session Paris (1996) paper 15/21/33-17

[153] Hoof, M.: Impulsfolgen-Analyse: Ein neues Verfahren der Teilentladungsdiagnostik. PH.D. Thesis University Siegen (1997)

[154] CIGRE TF 33.03.05: Calibration Procedures for Analog and Digital Partial Discharge Measuring Instruments. ELECTRA 180 (1998) pp. 123-124

[155] Kranz, H.G.: Fundamentals in Computer Aided PD Processing, PD Pattern Recognition and Automated Diagnosis in Gas Insulated Substations. IEEE Transactions on Electrical Insulation, Special Volta Issue (1999)

[156] Shim, I., Soraghan, J.J., Siew, W.H.: Digital Signal Processing Applied to the Detection of Partial Discharge: An Overview. IEEE Electrical Insulation Magazine, 16 (2000) 3, pp. 6-12

[157] Sahoo, N.C., Salama, M.M.A., Bartnikas, R.: Trends in Partial Discharge Pattern Classification: A Survey. IEEE Transactions on Dielectrics and Electrical Insulation, 12 (2005) 2, pp. 248-264

[158] Plath, R.: Multi-channel PD Measurements. 14th ISH Beijing (2005)

[159] Suresh, D.: Feature Extraction for Multi Source Partial Discharge Pattern Recognition. IEEE Indicon, Chennai, India (2005) pp. 309-312

[160] Kaufhold, M., Kalkner, W., Obralic, R., Plath, R.: Synchronous 3-Phase Partial Discharge Detection on Rotating Machines. Cigre Session Paris (2006) paper D1-105

[161] Eager, G.S., Bader, G., Heinrich, O.X., Suarez, R.: Identification and Control of Electrical Noise in Routine Reel corona Detection of Power cables. IEE Transactions on Power Apparatus and Systems, PAS-88 (1969) pp. 1772-1783

[162] Black, I.A.: A Pulse Discrimination System for Discharge Detection in Electrically Noisy Environments. 2nd ISH Zürich (1975) paper 32-02

[163] CIGRE WG 33.03: Elimination of Interference in Discharge Detection. ELECTRA 21 (1979) pp. 55–72

[164] Black, I. A., Leung, N. K.: The Application of the Pulse Discrimination System to Measurement of Partial Discharges in Insulation under Noisy Conditions. IEEE International Symposium on Electrical Insulation, Boston, MA (1980) pp. 167–170

[165] Borsi, H., M. Hartje, M.: New Methods to Reduce the Disturbance Influences on the In-situ Partial Discharge (PD)-Measurement and Monitoring. 6th ISH New Orleans (1989) paper 15.10

[166] Borsi, H.: New Method for Partial Discharges (PD) Location in High Voltage Cables under Noisy Condition. 7th ISH Dresden (1991) paper 75.05

[167]Kranz, H.G.: Diagnosis of Partial Discharge Signals using Neural Network and Minimum Distance Classification. IEEE Transactions on Electrical Insulation, EI 28 (1993) 6, pp. 1016-1024

[168] Wenzel, D., Schichler U., Bosri, H., Gockenbach, E.: Recognition of Partial Discharges on Power Units by Directional Coupling. 9th ISH Graz (1995) paper 5626

[169] König, G, Feser, K.: A New Digital Filter to Reduce Periodical Noise in Partial Discharge Measurements. 6th ISH New Orleans (1989) paper 43.10

[170] Nagesh, V., B.I. Gururaj, B.J.: Evaluation of Digital Filters for Rejecting Discrete Spectral Interference in On-site PD Measurements. IEEE Transactions on Electrical Insulation, EI-28 (1993) 1

[171] Köpf, U., K. Feser, K.: Rejection of Narrow-band Noise and Repetitive Pulses in On-Site PD Measurements. IEEE Transactions on Dielectrics and Electrical Insulation, 2 (1995) 6 pp. 1180-1191

[172] Buchalla, H., Flohr, T., Pfeiffer, W.: Digital Signal Processing Methods for Interference Recognition in Partial Discharge Measurement – A Comparison. IEE International Symposium on Electrical Insulation, Quebec (1996)

[173] Cavellini, A., Contin, A., Montanari, G.C., Puletti, F: Advanced PD Interference in On-Field Measurements, Part I: Noise Rejection. IEEE Transactions on Dielectrics and Electrical Insulation, Vol. 10 (2003) 6, pp. 216-224

[174] Cavellini, A., Contin, A., Montanari, G.C., Puletti, F: Advanced PD Interference in On-Field Measurements, Part 2: Identification of Defects in Solid Insulation Systems. IEEE Transactions on Dielectrics and Electrical Insulation, Vol. 10 (2003) 6, pp. 528-538

[175] Hettiwatte, S.N., Wang, Z.D., Crossley, P.A., Jarman, P., Edwards, G., Darwin, A.: De-noising of Partial Discharge Signals detected at a 400 kV Power Transformer. 13th ISH Delft (2003) paper P.02.11

[176] Happe, S., Kranz, H.-G., Krause, W.: Advanced Suppression of Stochastic Pulse Shaped Partial Discharge Disturbances. IEEE Transactions on Dielectrics and Electrical Insulation, 12 (2005) pp. 265-275

[177] Hayakawa, N., Sugimori, Y., Okubo, H.: Partial Discharge Current Pulse Waveform Analysis (CPWA) Based on Mechanisms in Solid and Gas Media. International Symposium on Electrical Insulating Materials, Kitakyushu, Japan (2005) pp. 812-815

[178] Sriram, S., Nitin, S., Prabhu, K.M.U., Bastiaans, M.J.: Signal De-noising Techniques for Partial Discharge Measurements. IEEE Transactions on Dielectrics and Electrical Insulation, 12 (2005) 6, pp. 1182-1191

[179] Kim, J.T., Kim, J.H., Koo, J.Y.: Noise Discriminations in Measuring Partial Discharges Using Pulse Wave Shape Analysis. CMD Changwon, Korea (2006)

[180] Cavallini,A. Montanari, G.C.: A Novel Method to Locate PD in Polymeric Cable Systems Based on Amplitude-frequency (AF) Map. IEEE Transactions on Dielectrics and Electrical Insulation Vol. 14 (2007) 3, pp. 726-734

[181] Mashikian, M.S., Bansal, R., Northrop, R.B.: Location and Characterization of Partial Discharge Sites in Shielded Power Cables. IEEE Transactions on Electrical Insulation, EI-5 (1990) pp. 883-839

[182] Steiner, J.P., Reynolds, P.H., Weeks, W.L.: Estimation the Location of Partial Discharges in Cables. IEEE Transactions on Electrical Insulation, EI-27 (1992) 1, pp. 44-59

[183] Wouters, P.A.F., van der Laan, P.C.T., Hetzel, E., Steenis, E.F.: New On-line Partial Discharge Measurement Technique for Polymer Insulated Cables and Accessories. 8th ISH Yokohama (1993) paper 6308

[184] Lemke, E., Schmiegel, P.: Complex Discharge Analyzing (CDA) – an Alternative Procedure for Diagnosis Tests on HV Apparatus of Extremely High Capacity. 9th ISH Graz (1995) paper 5617

[185] Gulski, E. Smit, J.J., Smit, J.C., Seitz, P.N., Turner, M.: On-site PD Diagnostics of Power Cables using Oscillating Wave Test System. 11th ISH London (1999) paper 5.112

[186] Lemke, E., Strehl, T., Boltze, M.: Advanced Diagnostic Tool for PD Fault Location in Power Cables Using the CDA Technology. 13th ISH Bangalore (2001) paper 6-72

[187] Gulski, E., Lemke, E., Gamlin, M. Gockenbach, E., Hauschild, W., Pultrum, E.: Experiences in Partial Discharge Detection of Distribution power Cables Systems. CIGRE WG-D1.33, ELECTRA 35, No. 208 (2003) pp. 35-43

[188] Lemke, E., Gulski, E., Hauschild, W., Malewski, R., Mohaupt, P. Muhr, M., Rickmann, J., Strehl, T., Wester, F.J.: Practical Aspects of the Detection of Partial Discharges in Power Cables. CIGRE WG D1.33.05, Technical Brochure 297, ELECTRA 63 (2006) pp. 63-70

[189] Baehr, R., Breuer W., Flottmeyer, F., Kotschnigg, J., Muller, R., Nieschwietz, H.: Diagnostic Techniques and Preventive Maintenance Procedures for Large Transformers. CIGRE Session Paris (1982) paper 12-13

[190] Fuhr, J., Haessig, M., Fruth, B., Kaiser, T.: PD Fingerprints of some High Voltage Apparatus. IEEE International Symposium on Electrical Insulation, Toronto (1990)

[191] Pietsch, R, Gutfleisch, Niemeyer, L.: Sequential Partial Discharge Pattern Analysis as a Diagnostic Tool for PD-Monitoring in HV Systems. Nordic Insulation Symposium, Bergen (1996)

[192] Stone, G.C.: Partial Discharge Signal Measurements to Assess Rotating Machine Insulation Condition: A Survey. IEEE International Symposium on Electrical Insulation, Montreal (1996)

[193] Wenzel, D., Borsi, H., Gockenbach, E.: A new Approach for Partial Discharge Recognition on Transformers On-site by Means of Genetic Algorithms: IEEE International Symposium on Electrical Insulation, pp. 57-60, Montreal 1996.

[194] Malewski, R., Feser, K., Claudi, A., Gulski, E.: Digital Technique for Quality Control and In-service Monitoring of HV Power Apparatus. CIGRE JWG 15/21/33-03, CIGRE Session Paris (1996)

[195] CIGRE JWG 15/21/33-02: Progress on High-Voltage Monitoring Systems for In-service Power Apparatus. CIGRE Session Paris (1996)

[196] Aschwanden, T., Hässig, M., Der Houhanessian, V., Zaengel, W., Fuhr, L., Lorin, P., Schenk, A., Zweiacker, P., Piras, A., Dutoit, J.: Development and Application of new Condition Assessment Methods for Power Transformers. CIGRE Session Paris (1998) paper 12-207

[197] Leibfried, T: Monitoring von Leistungstransformatoren - Jetzt auch für kleine und mittlere Baugrößen. Elektrizitätswirtschaft 98 (1999) 20

[198] Boss, P., Lorin, P., Viscardi, A., Harley, J.W., Iseke, J: Economical Aspects and Practical Experiences of Power Transformer On-line Monitoring. CIGRE Session Paris (2000) paper 12-202

[199] Borsi, H., Matthes, H., Poittevin, J., Sunderman, U., Tenbohlen, S., Uhde, D., Werle, P.: Enhanced Diagnosis of Power Transformers using On- and Off-line Methods - Results, Examples and Future Trends. CIGRE Session Paris (2000) paper 12-204

[200] Binder, E., Draxler, A., Egger, H., Hummer, A., Fuchs, H.R., Koklek, H. Müller, F. Drpic, M., Hof, M. Käfer, R., Lanz, S.: Entwicklungen und Nachweis-Untersuchungen von Diagnosemethoden für Wasserkraftgeneratoren. E&I 117 (2000) 12

[201] Hoof, M., Laird, T., Marsh, C.A.: Real-time Assessments Condition Trending of Generators Utilizing Continuous Partial Discharge Monitoring. EPRI-Utility Generator Predictive Maintenance and Refurbishment, New Orleans (2001)

[202] Hoof, M., Stephan, C.E.: Moderne Diagnoseverfahren zur Beurteilung der Wicklungsisolation elektrischer Maschinen. 46th Internationales Wissenschaftliches Kolloquium TU Ilmenau (2001)

[203] Strehl, T., Lemke, E., Elze, H.: On-line PD measurement, Diagnostic Tools and Monitoring Strategy for Generators and Power Transformers. 12th ISH Bangalore (2001)

[204] Lemke, E., Gockenbach, E. Kalkner, W.: Messtechnik für die Diagnose elektrischer Betriebsmittel. ETG-Fachtagung Diagnostik elektrischer Betriebsmittel, Berlin (2002) paper 4, pp. 25-29

[205] Plath, K.D., Plath, R. Emanuel, H., Kalkner, W: Synchrone dreiphasige Teilentladungsmessungen an Leistungstransformatoren vor Ort und im Labor. ETG-Fachtagung Diagnostik elektrischer Betriebsmittel, Berlin (2002) paper 11, pp 69-72

[206] Hudon, C., Belec, M., Contin, A., Cavalini, A., Nguyen, D.N., Montanari, G.C., Conti, M: Evolution in Automatic Phase Resolved Partial Discharge Pattern Recognition for Machine Diagnosis. 13th ISH Delft (2003) paper O.14.06

[207] Borsi, H., Gockenbach, E.: Partial Discharge Measurement and Evaluation Techniques for Transformers. 13th ISH Delft (2003) paper O.24.05

[208] Werle, P., Akbari, A., Gockenbach, E., Borsi, H.: An Enhanced System for Partial Discharge Diagnosis on Power Transformers. 13th ISH Delft (2003) paper P.11.09

[209] Claudi, A., Berlijn, S., Hauschild, W., Kocis, L., Lemke, E. Malewski, R.: Instrumentation and Measurements for In-service Monitoring of High Voltage Insulation. CIGRE WG D1-33.08, ELECTRA (2004)

[210] Hoof, M.: TE-on-line Monitoring an rotierenden Maschinen, Moderne Verfahren, Möglichkeiten und Grenzen der Zustandsbewertung. HIGHVOLT Kolloquium (2003) pp. 225-232

[211] Markalous, S., Huber, R., Tenbohlen, S.: On-site Teilentladungsmessung an Leistungstransformatoren. ETZ (2005) 1, pp. 42-44

[212] Kaufhold, M., Kalkner, W., Obralic, R., Plath, R.: Synchronous 3-Phase Partial Discharge Detection on Rotating Machines. CIGRE Session Paris (2006) paper D1-105

[213] Knowledge Rules for Partial Discharge Diagnosis in Service. CIGRE JWG-TF 15.11/33.03.02, Technical Brochure 226 (2003)